

**A STUDY OF FRACTAL ANALYSIS AND SINGULARITY SPECTRUM AND  
ITS POTENTIAL APPLICATION IN THE OIL AND GAS INDUSTRY**

By

SANDEEP RAMAKRISHNAN

FINAL PROJECT REPORT

Submitted to the Department of Electrical & Electronic Engineering  
in Partial Fulfillment of the Requirements  
for the Degree  
Bachelor of Engineering (Hons)  
(Electrical & Electronic Engineering)

Universiti Teknologi PETRONAS  
Bandar Seri Iskandar  
31750 Tronoh  
Perak Darul Ridzuan

# **CERTIFICATION OF APPROVAL**

## **A STUDY OF FRACTAL ANALYSIS AND SINGULARITY SPECTRUM AND ITS POTENTIAL APPLICATION IN THE OIL AND GAS INDUSTRY**

by

Sandeep Ramakrishnan

A project dissertation submitted to the  
Department of Electrical & Electronic Engineering  
Universiti Teknologi PETRONAS  
in partial fulfilment of the requirement for the  
Bachelor of Engineering (Hons)  
(Electrical & Electronic Engineering)

Approved:

---

Prof. Ir. Dr. Ahmad Fadzil M Hani  
Project Supervisor

UNIVERSITI TEKNOLOGI PETRONAS  
TRONOH, PERAK

December 2012

## **CERTIFICATION OF ORIGINALITY**

This is to certify that I am responsible for the work submitted in this project, that the original work is my own except as specified in the references and acknowledgements, and that the original work contained herein have not been undertaken or done by unspecified sources or persons.

---

Sandeep Ramakrishnan

## ABSTRACT

The world is made up of various irregular objects and signals. Although traditional mathematical techniques are not able to analyse these signals, it has been identified that these signals show common features such as singularities at various scales of observation. This indicates the existence of fractals within these signals. In the oil and gas industry, seismic data is a collection of reflected audio signals and is an example of irregular signals that could also have fractal features.

Even though we know that global petroleum resources are on the decline, oil and gas still remains the main source of energy throughout the world. This makes seismic exploration activities all the more important. Present indirect hydrocarbon detection techniques using seismic are costly and do not guarantee detection of oil or gas. Therefore, a technological advancement in the field of seismic exploration is evidently needed. Therefore, this study aims to develop a method for direct detection and delineation of hydrocarbons from seismic data.

In order to analyse the fractal nature of signals, a collection of mathematical steps known as fractal analysis is applied to generate a singularity spectrum. Although importance has been given on the methods of computing the singularity spectrum, there is little study on the effects of different types of singularities on the singularity spectrum. This study aims to understand how the singularity spectrum is affected by changes applied to input signals. It is by acquiring this knowledge first that the study also intends to develop an algorithm for direct detection of hydrocarbons. The Fraclab toolbox in MATLAB will be extensively used to achieve both of these goals.

From the study of the changes to singularity spectrum due to change in signals, it was observed that the square wave is the most irregular signal when compared with sine wave and sawtooth wave. Meanwhile, it was also discovered that a change in the amplitude of the periodic signal does not play a part in the final result of the singularity spectrum. The study has also observed that when two regular waves concatenate, the singularity spectrum produces more than one point due to the existence of a singularity or singularities at the point where the two signals concatenate. In direct comparison, when two periodic signals are added to one another, they only produce a dot on the singularity spectrum indicating that the end signal is still monofractal.

Seismic modelling revealed some promising results that could be translated into the development of a hydrocarbon detection method directly from seismic data. The seismic signals of three reservoir fluids that were modelled, namely oil, gas and water, resulted in different singularity spectra. It was observed that even when some features of the seismic model such as thickness of layers and number of layers were changed, the singularity spectrum produced by a particular reservoir fluid is the same. This means that each reservoir fluid has its own signature and thus could possibly be detected directly from real seismic data.

Indeed this proved to be true when tested with real seismic data. The windowing based technique that was used together with fractal analysis was able to detect and delineate the hydrocarbons. A region of high irregularity depicted by the continuous wavelet transform indicated the presence of hydrocarbon regions. Then with the spectral attribute values of  $\alpha_{\text{peak}}$  and asymmetry delineation was found to be possible. Gas regions produced results with lowest  $\alpha_{\text{peak}}$  values in the region of  $-2.1381 \leq \alpha_{\text{peak}} \leq -1.9958$ . The spectra produced in the gas region also produced asymmetry values in the following range of values,  $0.916025 \leq \text{asymmetry} \leq 1.069975$ . There was also a certain range of limiting values that were observed in the oil region. For  $\alpha_{\text{peak}}$ , the values were within  $-1.71331 \leq \alpha_{\text{peak}} \leq -1.60587$  while the asymmetry constantly remained between 1.253554 and 1.269845. This indicates that delineation of hydrocarbon was successful and the values mentioned above can be used to differentiate between oil and gas from seismic data.

## **ACKNOWLEDGEMENTS**

I would like to thank my supervisor, Prof. Ir. Dr. Ahmad Fadzil Mohd Hani, for his guidance and advice on my research that has allowed me to come up with this final report. I would also like convey my thanks to him for proposing an interesting topic such as this one.

The help of Dr. Ibrahima Faye is also much appreciated. His willingness to go through the mathematics of fractal analysis with me was an important part in ensuring the success of this project.

Finally, I give my thanks to my parents who have been a source of encouragement throughout the course of this project.

## TABLE OF CONTENTS

LIST OF TABLES .....	ix
LIST OF FIGURES .....	x
CHAPTER 1 INTRODUCTION .....	1
1.1 Project Background .....	1
1.2 Problem Statement .....	4
1.3 Objectives and Scope of study .....	5
1.4 Significance of study .....	6
1.5 Feasibility of study .....	7
CHAPTER 2 LITERATURE REVIEW .....	8
2.1 Fractal Analysis .....	8
2.1.1 Fractals .....	9
2.1.2 Holder Exponents .....	10
2.1.3 Fractal Dimensions .....	11
2.1.4 Singularity Spectrum .....	11
2.2 Oil and gas and the importance of seismic exploration in its detection .....	13
2.3 Current Seismic based detection methods and problems or shortcomings affiliated to them .....	15
2.3.1 Indirect Hydrocarbon Detection Method .....	15
2.3.2 Direct Hydrocarbon Detection .....	18
2.4 Fractal Analysis using Wavelet Transform Modulus Maxima Method to compute the singularity spectrum .....	20
2.4.1 The Continuous Wavelet Transform (CWT) .....	22
2.4.1.1 Finding Modulus Maxima Points .....	23
2.4.1.2 Connecting Modulus Maxima Points to form Modulus Maxima Lines .....	24
2.4.2 Tracking maxima lines and computing partition function .....	25
2.4.3 Computing scaling exponent, $\tau(q)$ .....	26
2.4.4 Compute singularity spectrum using Legendre Transform ...	27
CHAPTER 3 METHODOLOGY .....	30
3.1 Project Activities .....	30
3.1.1 PHASE ONE – FYP1 .....	31

3.1.2 PHASE 2 – FYP 2 .....	32
3.2 Tools and Software Required .....	43
3.3 Gantt Chart and Key Milestones .....	44
CHAPTER 4 RESULTS AND ANALYSIS .....	45
4.1 Results and analysis of singularity spectrum for various signals ...	45
4.1.1 Type of signals.....	45
4.1.2 Amplitude .....	47
4.1.3 Adding noise in the form of triangular pulse to the signal ....	48
4.1.4 Concatenate two sine signals of different frequencies .....	50
4.1.5 Addition of two sine waves in the same time period.....	52
4.2 Results and analysis from seismic modelling .....	54
4.2.1 Response of singularity spectrum towards change in Reservoir Fluid .....	55
4.2.2 Response of singularity spectrum towards change in Reservoir Fluid .....	56
4.2.3 Response of singularity spectrum towards change in stratigraphy .....	57
4.2.4 Analysis of results from seismic modelling.....	57
4.3 Results and analysis from the testing of the direct detection and delineation method on actual seismic data .....	59
4.3.1 Detection of the reservoirs .....	60
4.3.2 Delineation of Reservoirs .....	62
4.3.2.1 Delineation of reservoir WX-1 .....	62
4.3.2.2 Delineation of reservoir WX-2.....	64
4.3.2.3 Delineation of reservoir WX-3.....	66
4.3.2.4 Delineation of reservoir WX-4.....	68
4.3.2.5 Delineation of reservoir WX-5.....	70
4.3.2.6 Delineation of reservoir WX-6.....	71
4.3.2.7 Summarising the results from delineation.....	72
CHAPTER 5 CONCLUSION .....	74
5.1 Conclusion.....	74
5.2 Recommendations for future work.....	77
REFERENCES.....	78
APPENDICES .....	82
APPENDIX A – MATLAB CODES .....	82

## LIST OF TABLES

Table 1: Density, Velocity and Acoustic Impedance of different subsurface layers (Khan, 2007) .....	34
Table 2: Singularity spectrum attributes for different reservoir fluids .....	56
Table 3: Singularity spectrum attributes for each reservoir fluid at different thicknesses .....	56
Table 4: Singularity spectrum attributes for different number of layers of gas .....	57
Table 5: List of reservoirs and reservoir fluid.....	59
Table 6: Spectral attributes of related windows .....	63
Table 7: Spectral attributes related to windows at the start of WX-2 .....	65
Table 8: Spectral attributes towards the end of reservoir WX-2.....	66
Table 9: spectral attributes of windows related to WX-3 .....	68
Table 10: Spectral attributes of windows in reservoir WX-4 .....	69
Table 11: Spectral attributes of the spectra for reservoir WX-5 .....	70
Table 12: Spectral attributes of the spectra for reservoir WX-5 .....	70
Table 13: Spectral attributes of the spectra for reservoir WX-6 .....	71

## LIST OF FIGURES

Figure 1: Diagram on the left depicts history of total oil consumption in the world from 1950-2008 while diagram on the right shows history of gas consumption in the world for the same period. (Al Salam & Al Baruni, 2009).....	3
Figure 2: (a) WTMM method first proposed (b) Improved method proposed for fractal analysis using WTMM (Faghfour and Kinsner, 2005) .....	12
Figure 3: Figure depicting decline in oil discovery (Magoon, 2000) .....	13
Figure 4: Wavelet attribute analysis on migrated seismic section (a) The original migrated section (b) WT decomposition at voice 7 coloured by WT phase attribute (c) WT decomposition at voice 11 by WT phase attribute. (Xiaogui & Scot, 1998).....	16
Figure 5: Comparison between the fractal-based algorithm and three algorithms from the literature. The fractal-based algorithm is able to pick the correct arrival time in all the traces while the other algorithms may occasionally show relevant errors. ....	17
Figure 6: (a) 8-Hz common frequency section. The low-frequency shadow just beneath the reservoir is the strongest event on the section (b) 12-Hz common frequency section. The low frequency shadow and the reservoir have comparable amplitude (c) 20-Hz section. The low frequency shadow is completely attenuated .....	19
Figure 7: (a) Wavelet transform for scale $\sigma = 1$ . Figure shows the analysing wavelet (blue) , narrow since it is at the lowest scale trying to capture high frequency components in the signal (yellow) that are similar to it (b) Wavelet transform repeated for scale $\sigma = 20$ . (Polikar, 2006).....	23
Figure 8: An example of the coefficients of the continuous wavelet transform pictured in colour form in FracLab with the legend denoting the coefficients' amplitude based on colours.....	23
Figure 9: With reference to the points in the middle in all the pictures above, modulus maximum points are the points that have a happy smiley while the ones with the sad smiley are not modulus maxima points (Staal, 1995) .....	24
Figure 10: An example taken from Evertsz, Berkner & Berghorn (1995), showing modulus maxima lines in dotted lines for the signal which can be seen on the top half of the plot.....	25
Figure 11: Partition function plot for different values of $q$ seen on the left. The bottom right plot shows the scaling exponent plot for a sine wave in FracLab. The top right corner is the singularity spectrum generated.....	26
Figure 12: An example of a singularity spectrum produced on FracLab. The dots have been added to show where the gradient, $q$ which is also the mass exponent changes.....	28
Figure 13: Flowchart of research methodology .....	30

Figure 14: Snapshot of Fraclab toolbox .....	32
Figure 15: Steps to develop seismic models .....	33
Figure 16: An example of the reflectivity series produced .....	35
Figure 17: (a) Ricker wavelet with 60Hz centre frequency (b) Reflectivity series after convolved with ricker wavelet.....	36
Figure 18: Flowchart of the steps involved in the Direct Detection and Delineation Algorithm.....	37
Figure 19: Synthetic seismogram of the well.....	38
Figure 20: Reflection coefficient and acoustic impedance .....	39
Figure 21: Upsampling process (Mohamad Hani, 1999).....	40
Figure 22: Upsampled seismic trace .....	41
Figure 23: (a) Real part of the Morlet wavelet (b) Imaginary part of the Morlet wavelet.....	42
Figure 24: (a) The sine wave used for this test, (b) Singularity spectrum produced for the sine wave.....	45
Figure 25: (a) Sawtooth wave used for this test, (b) Singularity spectrum produced for the sawtooth .....	45
Figure 26: (a) Square wave used for this test (b) Singularity spectrum produced for the square wave.....	46
Figure 27: (a) One of the sine waves used for this test (amplitude = 0.1) (b) Singularity spectrum produced was a dot and it was the same for all different amplitudes of the sine wave.....	47
Figure 28: (a) One of the sawtooth waves used for this test (amplitude = 1), (b) Singularity spectrum produced was the same for all different amplitudes of the sawtooth signal .....	47
Figure 29: (a) One of the square waves used for this test (amplitude = 1), (b) Singularity spectrum produced was the same for all different amplitudes of the square waves .....	47
Figure 30: (a) The green signal is the sine wave after noise (blue) is added to it, (b) Singularity spectrum produced for the signal in (a) .....	48
Figure 31: (a) The green signal is the sine wave after noise (blue) is added to it, (b) Singularity spectrum produced for the signal in (a) .....	49
Figure 32: (a) The green signal is the sine wave after noise (blue) is added to it, (b) Singularity spectrum produced for the signal in (a) .....	49
Figure 33: (a) 100Hz sine wave concatenated with a 10Hz signal, (b) Singularity spectrum produced.....	50
Figure 34: (a) 100Hz sine wave concatenated with a 40Hz signal, (b) Singularity spectrum produced.....	51

Figure 35: (a) 100Hz sine wave concatenated with a 50Hz signal, (b) Singularity spectrum produced.....	51
Figure 36: (a) 100Hz sine wave concatenated with a 60Hz signal, (b) Singularity spectrum produced.....	51
Figure 37: (a) A part of the 0.5 seconds long 100Hz sine wave (b) Singularity spectrum produced for the sine wave in (a).....	52
Figure 38: (a) 100Hz signal added to a 10Hz signal (b) Singularity spectrum produced for the sine wave in (a) .....	53
Figure 39: (a) 100Hz signal added to a 20Hz signal (b) Singularity spectrum produced for the sine wave in (a) .....	53
Figure 40: (a) 100Hz signal added to a 30Hz signal (b) Singularity spectrum produced for the sine wave in (a) .....	53
Figure 41: (a) 100Hz signal added to a 40Hz signal (b) Singularity spectrum produced for the sine wave in (a) .....	54
Figure 42: (a) Singularity Spectrum for Gas (b) Singularity Spectrum for Oil (c) Singularity spectrum for Water.....	55
Figure 43: A graphical illustration of the steps to obtain windows .....	60
Figure 44: $\alpha_{\text{peak}}$ plot of all the windows .....	61
Figure 45: Continuous wavelet transform with the regions where gas and oil are present. Gas reservoirs are highlighted by the black boxes while oil reservoir is highlighted by the red box .....	61
Figure 46: Singularity spectrum of windows 54, 55 and 56 .....	62
Figure 47: Window 55 or WX-1 .....	63
Figure 48: Singularity spectrum of windows 73, 72 and 71 .....	64
Figure 49: Singularity spectrum of windows 81, 80 and 79 .....	65
Figure 50: Singularity spectrum of windows 107, 108 and 109 .....	67
Figure 51: Singularity spectrum of window 108.....	67
Figure 52: Singularity spectra of windows 162-164.....	69
Figure 53: Singularity spectra of windows 237, 238 and 239.....	70
Figure 54: Singularity spectra of windows 91, 92 and 93.....	71

# CHAPTER 1

## INTRODUCTION

### 1.1 Project Background

Natural objects like clouds or trees and signals like lightning strikes very rarely have a linear pattern. To add on to that, in understanding any signal, it is common that the irregular patterns or spikes that contain the data that is important. Characterizing these objects or signals by traditional mathematical techniques has proven to be inaccurate. However from various studies, these nonlinear objects and signals indicate having a similar pattern on more than one scale and are characterized as fractals.

In order to understand the complex patterns of fractals, an analytical technique called fractal analysis that was developed not too long ago is used. This method has picked up popularity in recent times as it provides a way for irregular signals to be characterized. Applications of fractal analysis has grown and is currently being used in many fields like stock market modelling, image processing, medical data and networking (Reidi).

Through fractal analysis, fractal characteristics like holder exponents and fractal dimensions are generated. A holder exponent gives the degree of irregularity in a function while fractal dimension gives the degree to which a fractal object is fragmented. Having computed these values, a singularity spectrum can then be plotted to further quantify a non-linear signal. From previously being unable to analyse irregular signals accurately, developments in fractal analysis now enable accurate analysis of complex signals and at the same time allow for classification of these signals under common features like holder exponents and fractal dimensions.

The evidence that even irregular signals have distinct characteristics generated interest in studies on holder exponents and fractal dimensions. Scientific papers that focused on holder exponents aimed at using holder exponents for singularity detection. The common method used in these studies to obtain holder exponents is by using wavelet transform (Sohn, Robertson & Farrar, 2002, Mallat & Wen, 1992).

Wavelet transform is a very important mathematical tool in studying the regularity of a signal because it is able to localize a signal in both time and frequency at the same time. This was a major improvement from the traditional technique of Fourier transform as wavelet transform was capable of giving the local regularity of signals in comparison to Fourier transform which gives the overall regularity of a signal.

Meanwhile, many researchers have also taken fractal dimension as an important feature in defining complex signals. For instance two different approaches by which fractal dimensions can be obtained were studied and compared in the study by Backes and Bruno (2008) although the focus was on the study of complexity of shapes. Fractal dimensions have been used to characterize various complex natural features like the shape of soils and rocks, the blood vessels in the human body and how they branch out and the sometimes the distribution of plants (Jonckheere, Nackaerts, Muys, Aardt & Coppin, 2006).

Putting these two features - namely holder exponents and fractal dimensions - of an irregular signal together in one plot gives rise to the singularity spectrum. Extensive studies have been undertaken in order to identify and describe the steps in carrying out fractal analysis to produce a singularity spectrum (Chhabra et al., 1989, Arneodo, Bacry & Muzy, 1995). Furthermore, with the aim of improving the accuracy of the singularity spectrum produced, the study done by Faghfour and Kinsner (2005) has also provided some solutions to address the challenges previously faced in the computation of a singularity spectrum.

As mentioned previously, fractal analysis is now gaining popularity in many fields. The oil and gas industry is another important field where fractal analysis can be implemented. At the moment, the world relies heavily on oil and gas as energy sources. As mentioned in by Al Salam and Al Baruni (2009), 39% of the energy needs across the world is provided by petroleum while another 23% was contributed by gas. As seen in the figures below, the consumption of oil and gas has always been on the rise.

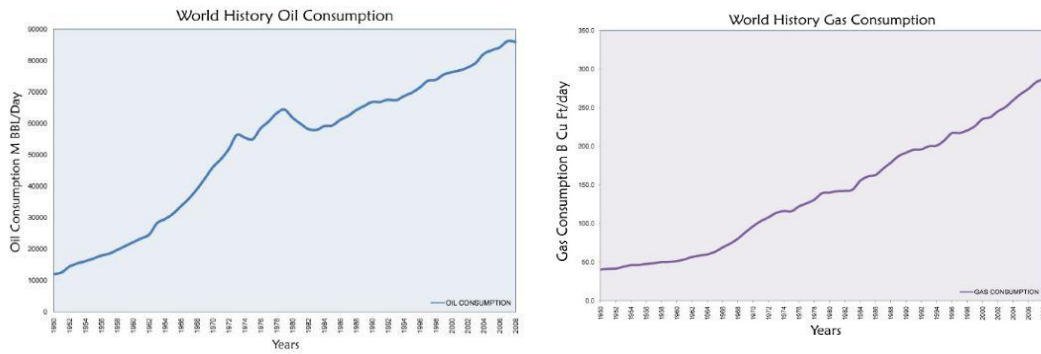


Figure 1: Diagram on the left depicts history of total oil consumption in the world from 1950-2008 while diagram on the right shows history of gas consumption in the world for the same period.

(Al Salam & Al Baruni, 2009)

It is predicted that this trend will continue and the global use of petroleum will grow by another 5% in the first twenty five years of the 21<sup>st</sup> century. Meanwhile, it is also predicted that natural gas will face a massive increase in consumption with an expected increase of 57% in the same time frame. These trends are worrying as it will lead to a situation where the demand is higher than the supply made available by energy companies (Al Salam & Al Baruni, 2009).

Therefore, the need for better technologies in the exploration of oil and gas has never been more evident. This is because oil and gas exploration is usually the most vital step as it determines if the area under study has hydrocarbon in amounts that are economically profitable to be extracted ("Oil and gas,"). After detailed analysis of geological maps to locate major sedimentary basins is completed, further information is gathered by commissioning field geological assessments ("Environmental management in," 1997).

Three of the most common methods in conducting these assessments are magnetic, gravimetric and seismic. The changes in strength of the magnetic field are recorded in the magnetic method. With this information, the type of the rocks present can be identified by looking at their magnetic characters. Meanwhile, the gravimetric technique detects and records minor changes in the gravitational field at the surface of the earth. These measurements are made either by using an aircraft or a survey ship ("Environmental management in," 1997).

Nevertheless, of the three methods, seismic surveys are considered the most important and are usually the first field activity undertaken. This method uses sound waves in order to produce an image of the subsurface geological structures and layers.

An energy source usually an airgun is used to transmit acoustic energy that travels into the earth in the form of a wave. Each time the wave comes into contact with a different layer, some of the energy is reflected back to the surface. At the surface, an array of receivers - geophones on land or hydrophones in water – pick up the reflected sound waves for processing. The rest of the energy on the other hand continues down to detect the geological strata that exists deeper within the earth ("Oil and gas," "Environmental management in," 1997).

Once the seismic surveys are conducted, the information gathered needs to be processed. Various signal processing methods come into play at this stage. Data processing is important as it reduces the effects of common problems like noise or multiples. Multiples occur when the same layer reflects the sound wave repeatedly ("Discovering the underground,"). Processing seismic data also includes enhancing the signals and migrating the seismic events to its actual location in space (Albertin et al. 2002). Processing of seismic data is vital as this usually sets the tone for geophysicists to interpret the data effectively in order to determine the possible presence of hydrocarbon zones.

Since seismic data is non-linear, the possibility of using fractal analysis to analyse the data has been an area of study that has interested some scientists. Wilson (n.d.) for instance made an attempt to identify the fractal interrelationships in field and seismic data. Khan (2007) went a step further by using fractal analysis to detect and delineate hydrocarbons. This study sets out to consolidate these findings in applying fractal analysis in the detection of hydrocarbons.

## **1.2 Problem Statement**

Since fractal analysis is a relatively new area of study, there is a lot still to be learned about the characteristics of a fractal signal like fractal dimensions and holder exponents. Although importance has been given on the methods of computing the singularity spectrum, the studies have stopped short of explaining the effects of different types of singularities on the singularity spectrum. In other words, a lot of effort has been put into perfecting the methods involved in fractal analysis to generate a singularity spectrum but little is known on how various characteristics of signals or changes in signals affect the values obtained in a singularity spectrum.

Therefore, this study sets out to analyse different signals using fractal analysis and observe changes on the singularity spectrum in order to correlate different singularities to their effects on the singularity spectrum. It is then hoped that the data obtained can be explained with the mathematics behind fractal analysis.

At the present time where hydrocarbon resources are on the decline, the exploration for new oil and gas reservoirs is very important. In the hydrocarbon exploration field, seismic surveys play a major role in the detection of hydrocarbons. A lot of signal processing is done to the information gathered to enable proper interpretation of the seismic data. In interpreting seismic data, there are both indirect and direct methods of hydrocarbon detection (Khan, 2007).

Indirect hydrocarbon detection needs more than just seismic surveys in order to be able to detect hydrocarbons. Through this method, the seismic geological models have to be improved by physically detecting the oil and gas deposits by obtaining core samples (Khan, 2007). Due to this, wells have to be drilled and as a result a lot of money is consumed. This method is also time consuming as well logs have to be matched to the seismic data so that an accurate geological model can be made. Once this model has been made, whether or not oil and gas is present in an economically viable amount depends on the proper interpretation of the formation geology (Avseth, Mukerji & Mavko, 2005).

Direct hydrocarbon detection is also currently in practice. This method only analyses the frequency components of the seismic data (Khan, 2007). This method is undeniably faster than the indirect hydrocarbon detection method. However, with the development of fractal analysis, irregular signals can now be quantified. This opens up the possibility of improving the effectiveness of direct detection method using seismic data as the singularity spectrum characterizes the signals in a more detailed manner. Therefore, this paper attempts to develop a direct hydrocarbon detection method using fractal analysis for improved hydrocarbon detection.

### **1.3 Objectives and Scope of study**

Fractal analysis has proven that it is an important signal processing tool with its ability to detect local and global transitions. The first objective of this study is to analyse the fractal analysis performed on generated signals. This would be the interim objective that is hoped to be achieved in the first semester. The main feature of fractal

analysis that is under study would be the singularity spectrum. The study plans to investigate the changes on singularity spectrum as the input signals are varied. Various characteristics of the signals will be changed like signal amplitude, number of cycles of each signal and type of signals to name a few. These signals will be analysed using the FracLab toolbox. FracLab is a general purpose signal and image processing toolbox based on fractal and multifractal methods.

Since fractal analysis is made up of a set of mathematical steps, the study also aims to relate the changes observed in the singularity spectra produced in FracLab with the mathematics behind the analysis. Through such an analysis on the singularity spectrum, which signal is considered more singular can be identified. Also, the reason why some signals are said to be more singular than others can be explained by matching the results obtained in the singularity spectra to the mathematics behind the analysis.

The major objective of this study is to come up with a method for direct detection of hydrocarbons. Seismic surveys are done in the early stages of oil and gas exploration and whether a reservoir is profitable for production many times depends on the seismic data. Therefore, this study aims to use the singularity spectrum generated using fractal analysis to develop an algorithm for direct detection of hydrocarbons. Since it is a direct method, conclusions can be drawn on a reservoir just by interpreting the seismic data. Furthermore, this proposed method should have an improved reliability as compared to the current direct method in use. Also, the proposed method would not need for an exploration hole to be drilled meaning millions of dollars could be saved in the exploration stage.

#### **1.4 Significance of study**

The discontinuities in a signal contain the most important information of that particular signal. Although for a very long time, Fourier transform has been the main approach in the study of singularities of a signal, the developments in fractal analysis has shown that fractal analysis provides a better way to characterize and understand irregular signals. Since most studies have focused on the applications of fractal analysis, the understanding on the types of singularities and their effects on the singularity spectrum seems to have been overlooked. Therefore, through this study a

clearer picture on the effects of changing the characteristics of a signal on the singularity spectrum can be obtained.

Currently, fractal analysis has been applied in some studies related to geological studies. For instance Hermann and Lyons (2000) have classified stratigraphy and lithology of the earth by using singularity analysis. However there are few studies on how fractal analysis can be used on seismic data for direct detection of hydrocarbons. The proposed method of hydrocarbon detection by analysing the singularity spectrum and characteristics like holder exponents and fractal dimensions give a more reliable way of hydrocarbon detection as compared to present methods. This is because the present method only looks at the frequency changes in the seismic data to predict presence of hydrocarbons.

### **1.5 Feasibility of study**

The aim of the study at the end of both phases (FYP1 and FYP2) is to create an algorithm that can be used for direct detection of hydrocarbons. The main task that needs to be covered in order to reach this ultimate goal is to understand fractal analysis. Since this task would be achieved in the first phase, there would be sufficient time to use the knowledge gained to formulate an algorithm for direct hydrocarbon detection of hydrocarbons from seismic data in the second phase. Nevertheless, to validate the capability of the fractal analysis method in detecting hydrocarbons, it is vital that actual seismic data is obtained from PETRONAS so that the algorithm created can be compared with actual data from the field to proof its reliability.

## CHAPTER 2

### LITERATURE REVIEW

#### 2.1 Fractal Analysis

Albeit being a relatively new mathematical approach towards analysing signals, fractal analysis has already found widespread interest due its ability to categorize irregular signals. In this chapter, some of the works already done on fractal analysis are discussed in relation to the interim aim of this study. Also, studies on the characteristics of complex signals like holder exponents, fractal dimensions and singularity spectrum are looked into for further understanding. Since the final objective of the study is to apply fractal analysis for detection of hydrocarbons, studies that have applied fractal analysis on seismic data or in the field of geology are discussed too.

There are many types of nonlinear and nonstationary signals both in time and space like electrocardiogram (ECG), electroencephalogram (EEG) , network traffic , physiological responses and lightning strikes to name a few. However as mentioned in a few studies, common spectral methods like Fourier Transform or other traditional signal processing methods are incapable of analysing these signals (Faghfour & Kinsner, 2005, Chakraborty & Okaya). This is true since Fourier Transform assumes the signal to be stationary. Therefore, from the frequency spectrum produced, the exact time at which different frequencies or singularities occur cannot be ascertained.

However with the developments in wavelet transform (WT), it was now possible to extract both frequency and time factors of a signal simultaneously. This opened up the possibility of identifying singularities at its exact moment of occurrence. WT was then used as a basis towards developing an approach called fractal analysis that can categorize irregular signals.

Khan (2007) and Reidi have mentioned that fractal analysis is an approach that is able to capture the long-term dynamical behaviour and statistical self-similarity of the

aforementioned signals. Meanwhile, fractal analysis has also been defined as a collection of mathematical steps that are used in order to identify fractal dimensions or other fractal characteristics like Holder exponents (Zmeskal, Vesely, Nezadel & Buchniecek, 2001). In essence, these studies are in agreement that with fractal analysis, the sudden changes or singularities of a signal can be identified and characterized using Holder exponents and fractal dimensions. Fractal analysis also generates a singularity spectrum that gives a mean for quantifying the complex signals further (Faghfour & Kinsner, 2005). The singularity spectrum computed by fractal analysis is a major part in this study as it aims to understand how the quantization is done. Nevertheless, before discussing on studies that have dealt with singularity spectrum, this study first describes some terms that are important and used throughout this study.

### ***2.1.1 Fractals***

The word fractal relates to highly irregular patterns, shapes and mathematical sets (Khan, 2007). One way to describe fractals is that the object or fractal contains smaller versions of itself (Weisstein). The concept of characterizing space-time by four Euclidean integer changes with the introduction of fractals since with fractals, complex shapes can have dimensions that are fractions. (Kinsner, 2005)

Regular or deterministic fractals are objects or quantities that exhibit self-similarity on all scales (Weisstein, Dansereau & Kinsner, 2001, Khan, Mohamad Hani, Firdaus & G., Evertsz, Berkner & Berghorn, 1995). Self-similarity means that the object would have the same features on any scale. It is also important to note that in order for something to be a regular fractal the scales used must be the same.

Meanwhile, self-affine fractals are objects that have a self-similar structure but at different scales (Khan, Mohamad Hani, Firdaus & G.). For instance, if there exists a signal  $y(t)$  with an independent variable  $t$ , then the signal would be self-affine if the scaling on the amplitude of  $y(t)$  is different from the changes to the scale of the variable  $t$  (Faghfour & Kinsner, 2005). Some examples of self-affine fractals are seismic data, retinal vessels and network traffic.

Fractals could be seen in two categories, namely monofractals and multifractals. Fractals that have one fractal dimension are known as monofractals. Meanwhile

functions are called multifractals are if there are more than one fractal dimension to describe it. (Kinsner, 2005, Khan, 2007)

### ***2.1.2 Holder Exponents***

Holder exponents or also known as Lipschitz exponents are used to obtain the local measure of regularity of a function (Jouck, 2004, Mallat & Wen, 1992). The singularities and irregular structures of a function are of importance since most of the vital information that defines the function lie within them (Mallat & Wen, 1992). Holder exponents can take positive or negative values where smaller values mean the strength of the singularities is higher. (Staal, 1995)

Fourier Transform used to be the main technique used to analyse singularities in signals or functions. However, Fourier transform (FT) is a global analysis of the regularity of the signals and assumes the function to be stationary. Since FT produces an analysis of only frequencies and does not specify the time when the frequencies occur, the exact location of singularities could not be identified (Mallat & Wen, 1992).

One mathematical approach that solves the problems found in FT is wavelet transform (WT) as it can characterize the local regularity of signals (Mallat & Wen, 1992). WT gives the time and frequency content of functions simultaneously. (Polikar, 2006) Through this method, the exact time and the exact frequency of the singularity can be obtained. This is exactly what is needed to analyse singularities in a signal.

An interesting feature of wavelets that is of importance is its ability to adapt its width to the frequency (Polikar, 2006, Jouck, 2004). The wavelets produced are narrow for high frequency components whereas at lower frequencies the wavelets are wider. Due to this feature in wavelets, wavelet transform allows for better understanding of high frequency changes or singularities as the resolution of the analysis at high frequency is very high (Polikar, 2006, Jouck, 2004). As mentioned earlier, since important information regarding a signal is stored in the singularities, this is a favourable feature of WT in relation to the study.

In this study, the tracking of local maxima of WT together with the use of modulus-maxima lines is the fundamental methods involved in identifying the holder

exponents. This method is called the Wavelet Transform Modulus Maxima (WTMM) (Evertsz, Berkner & Berghorn, 1995).

### ***2.1.3 Fractal Dimensions***

The study of the complexity of a function is one of the common ways in analysing it. The complexity of a function relates directly to the irregularity of the function. One of the methods in determining the complexity of an object or signal would be through fractal dimension. Fractal dimension gives information on how fragmented a fractal object is or in other words it is a characterization of the self-similarity of the fractal (Mandelbrot, 2000). Unlike topological dimension, fractal dimension provides a non-integer value that quantifies how much of the fractal is found in the space under observation (Backes & Bruno, 2008).

However, not all objects or functions in nature are self-similar. Therefore, a single numeric value is not enough to describe the complexity of these fractals. In the 1970s, Mandelbrot iterated that objects that are self-affine should be characterized by a spectrum of numbers instead of just one dimension (Kinsner, 2005). This led to the use of Multi-Scale Fractal Dimension (MFD) method which uses more than one scale to quantify the density of fractals in a metric space. From here more than one fractal dimension values are obtained these values will then be used in the formation of a singularity spectrum.

### ***2.1.4 Singularity Spectrum***

The statistical properties of the singular exponents or holder exponents are described through a singularity spectrum (Chhabra, Meneveau, Jensen & Sreenivasan, 1989). A singularity spectrum is used to quantify the degree of irregularity of fractals. For monofractals, the singularity spectrum would only produce one dot while multifractal signals would produce a spectrum with all of its holder exponents and fractal dimensions (Faghfour & Kinsner, 2005). The reason for monofractals producing a single point on the singularity spectrum is due to the fact there is only one fractal dimension and holder exponent to describe them.

With the understanding of these terms, our study looks at some of the researches that have focused on fractal analysis as well as singularity spectrum. Faghfour and

Kinsner (2005) described that there are two important methods in computing a singularity spectrum namely the Legendre transform of the Renyi fractal dimension spectrum while the second method is by using the Wavelet Transform Modulus Maxima (WTMM). The study then proceeds to discuss the WTMM method in detail and providing methods to improve the reliability of the method which was proposed in an earlier study by minimizing errors and reducing noise as seen in their flowchart below. There are also other studies that have also used WTMM to produce the singularity spectrum like Khan (2007) and Los and Yalamova (2006). This study will also be applying the WTMM method as it is found to be the method that is able to detect all the singularities in a signal. Therefore, similar steps can be adapted from these research papers to perform fractal analysis. Nevertheless, several different methods applied by others are mentioned in the following paragraph.

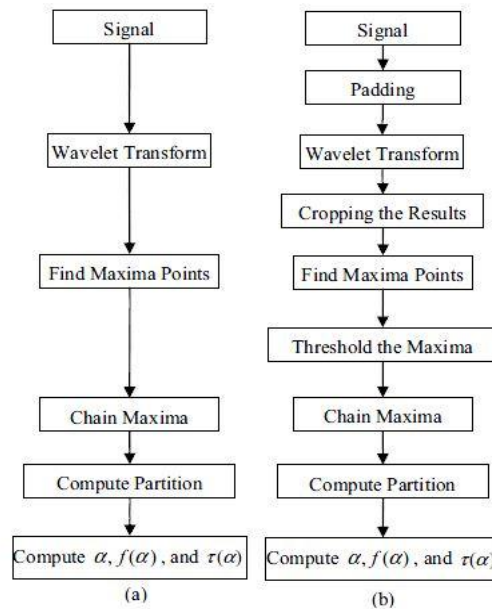


Figure 2: (a) WTMM method first proposed (b) Improved method proposed for fractal analysis using WTMM (Faghfour and Kinsner, 2005)

There is also a scientific paper that explains a direct method of computing a singularity spectrum from the experimental data (Chhabra et al., 1989). The follow up to the study was the application of this fractal analysis method on fully developed turbulence. This is a method that is different compared to the WTMM method since the need of Legendre transform as one of the steps in obtaining the singularity spectrum is effectively removed. Another study proposed a method called the method of moments to compute (Bobrov et al.). This is another method that has been

proven to be able to generate a singularity spectrum. The method was then applied in the geophysics field to investigate non-stationary properties of geophysical processes.

## 2.2 Oil and gas and the importance of seismic exploration in its detection

Oil and gas are the two main energy sources that meet more than half of the global energy demand. In order to identify the reservoirs, oil and gas carry out exploration by using various methods. This section onwards will discuss on the major types of exploration methods involved. However, emphasis would be given towards seismic method. Therefore, current approaches as well as research developments in seismic surveying would be discussed as well.

Although oil and gas are non-renewable energies, there are little signs that the dependence towards these energy sources are on the decline as 63 percent of the world energy supply comes from these sources ("Environmental management in," 1997). It has also been pointed out that the volume of oil discovered around the globe every five years is on the decline (Magoon 2000). This can be observed in Figure 4 below.

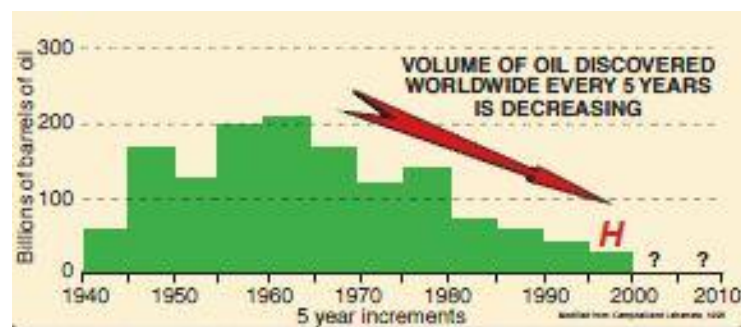


Figure 3: Figure depicting decline in oil discovery (Magoon, 2000)

This situation has increased the pressure on oil and gas companies to ramp up efforts in discovering more oil and gas reservoirs. Therefore, more money is pumped into research in order to develop present exploration technologies. Nevertheless, it is important to first have a general idea of the exploration methods that are currently employed.

Of the various exploration tools, the three major survey methods are magnetic, gravimetric and seismic. In a magnetic survey, information on the distortions in the Earth's crust is collected by a magnetometer that is towed by a boat. The aim of doing this is to identify subsurface traps. Subsurface rocks have their own magnetic

properties that can be measured using this method. From there, it can be identified if rocks that usually cause petroleum to move upward into subsurface traps like granite exist. Meanwhile, gravimetric method uses a sensor called gravimeter which measures the strength of the gravitational field. This exploration tool allows for detection of porous materials where petroleum could be found. Apart from that it also identifies the location of certain formations that usually trap hydrocarbons ("Oil and gas,").

Seismic surveying however is the most commonly used method as it is considered the best of the three. This process is carried out by sending sound waves into the earth's crust like the seabed for offshore operations. The time taken for the sound wave to be reflected back to the surface is recorded. This information enables geophysicists to come up with an image of the subsurface strata and structures. While some of the sound wave is reflected, the balance of the sound wave continues to travel deeper into the ground to detect other layers. Since seismic waves that are reflected off rock layers that are denser produce a different signal when compared to porous materials, exploration geophysicists can attempt to use this data to pinpoint the location of oil and gas reservoirs. The tools required to conduct a seismic survey is a sound source – typically an air-gun on a ship – and also receivers known as hydrophones which are towed by the ship ("Oil and gas," ). The three steps involved in seismic method are acquisition, processing and interpretation.

Traditionally in seismic surveying, seismic interpreters try to identify potential reservoirs by looking at structural and stratigraphic features that have previously proven to be of oil and gas reservoirs. Therefore, seismic interpretation depends a lot on experience and knowledge on the subject matter. Also, in these conventional techniques reservoir parameters were distinguished from one another by amplitude analysis. Also, these conventional methods have solely been used to detect hydrocarbons indirectly.

However with time, new technologies were developed to improve the reliability in detecting hydrocarbons. One such method is the amplitude versus offset (AVO) analysis. Albeit being an amplitude analysis method, it reduced interference in the amplitude caused by layers that were close to each other. This was also still an indirect hydrocarbon detection method from seismic data. The frequency content of the seismic data was also used to detect hydrocarbons via a method called spectral

analysis. The application of this method has seen a drastic increase of late (Maklad, 2007). The reason for this was due to the fact that this led to the possibility of direct hydrocarbon detection.

### **2.3 Current Seismic based detection methods and problems or shortcomings affiliated to them**

#### ***2.3.1 Indirect Hydrocarbon Detection Method***

In the indirect hydrocarbon detection method, the seismic attributes from a seismic survey is studied in order to gather data on the physical properties of the layers of rock within the ground. These properties range from the thickness of a layer down to the porosity of the rock in the layer. This enables the exploration geophysicists to come up with a geological model in order to identify possible locations of oil and gas reservoirs (Khan, 2007).

The AVO analysis is a common indirect detection method. Based on kind of seismic data in use, there are two types of AVO phenomena with the first one being P-wave AVO and the second one being multicomponent AVO. Before the use of AVO, high amplitude regions in seismic data were said to be an indication of gas based on practical evidence. However this was proven to be an unreliable method for predicting existence of gas since hard rocks also produced high amplitude regions in the seismic survey. AVO however was able to differentiate these two scenarios. This was due to the high levels of sensitivity of the P-waves towards gas sandstones thus producing high amplitude reflections for those regions while low amplitudes for every other region. Since AVO produces reliable results only when the sand to shale impedance contrast is high, it has its limitations (Li et al., 2007, Fatti et al., 1994). Therefore in order to confirm the presence of hydrocarbons, after the seismic survey is conducted and analysed using AVO, a well is drilled and other exploration tools are used to gather more data.

A study that uses wavelet transform as the basis of its research on estimating Q attenuation is by Xiaogui and Scot (1998). Q is the ratio between the peak energy of a wave to the energy that is dissipated. When performing seismic interpretations, this energy loss must be taken into account. Their study uses Wavelet Transform Modulus spectra and Matching Pursuit Decomposition spectra to estimate the Q attenuation.

Matching Pursuit Decomposition performs signal decomposition using more than one type of wavelet to get a high resolution analysis. This research has proven to be able to provide higher accuracy for Q function estimates. This will help in the process of fluid and lithological interpretations. While this method does provide an improvement in giving a better estimate of attenuation, just this data alone will not suffice in the detection of hydrocarbons. However, this study shows a shift towards a growth in the application of wavelet transform in seismic analysis.

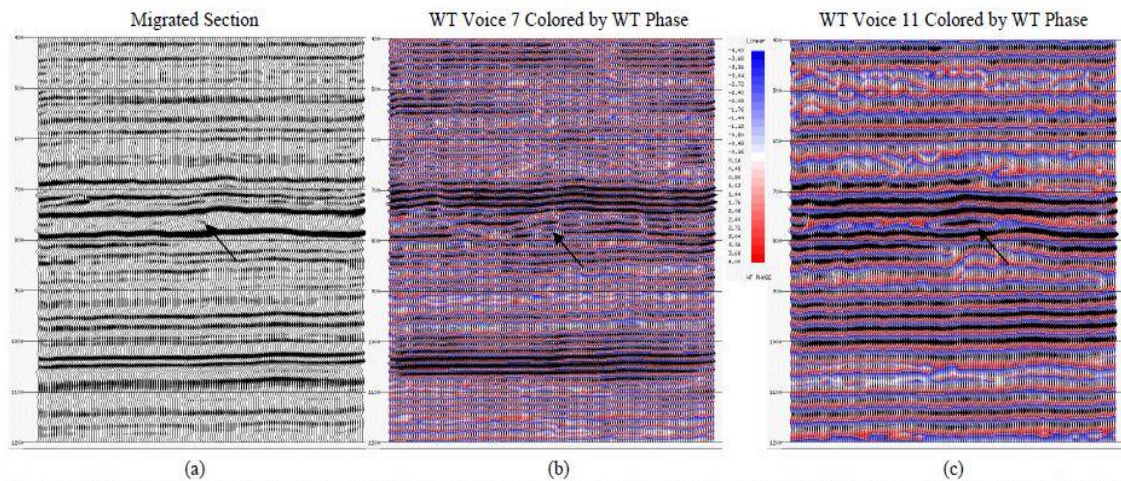


Figure 4: Wavelet attribute analysis on migrated seismic section (a) The original migrated section (b) WT decomposition at voice 7 coloured by WT phase attribute (c) WT decomposition at voice 11 by WT phase attribute. (Xiaogui & Scot, 1998)

In indirect hydrocarbon detection method based on seismic data, the travel time of seismic waves from the source to receiver needs to be determined with as minimal error as possible. This is crucial especially when the seismic-velocity structure of the subsurface are being identified. While there are many published algorithms to detect the seismic first arrival times, the fractal based algorithm proved to be able to tolerate noise levels up to 80% of the average signal amplitude. This study proves that using a fractal dimension as an indicator improves accuracy of data. It is a sign that using fractal-based attributes provide better results. (Boschetti, Dentith & List, 1996)

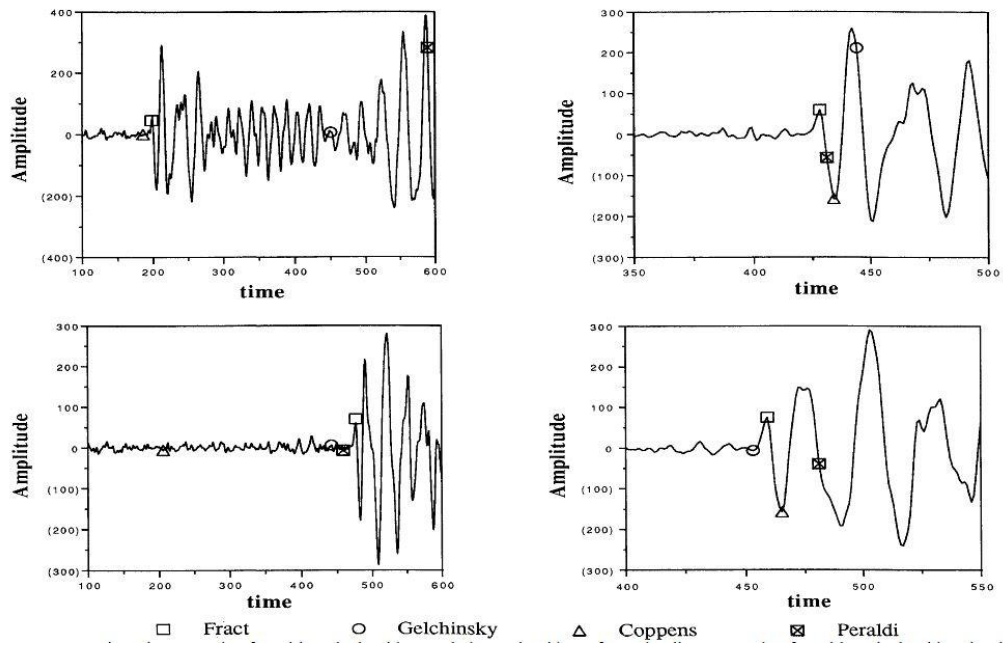


Figure 5: Comparison between the fractal-based algorithm and three algorithms from the literature. The fractal-based algorithm is able to pick the correct arrival time in all the traces while the other algorithms may occasionally show relevant errors.

Spectral decomposition is another analysis method that is becoming more common and it is used to break down the seismic data into its frequency components. This method has been used in studies in order to visualize the stratigraphy of the Earth. One of the reasons for this is down to the fact that spectral decomposition helps the geophysicist to get data on the small changes in thickness between layers. Even more important is its ability to give the exact thickness of the layers (Hall & Trouillot, 2004). This analysis method allows for interpreters to locate the stratigraphic trap which are possible signs of the presence of hydrocarbons. This is vital information when modelling the geological map. However, in this method there is no absolute way of saying if there are hydrocarbons present unless other well logging tools are used for verification.

Seismic thin bed analysis meanwhile is used to detect and quantify the thickness of these beds in seismic data. Frequency domain thin bed analysis of seismic data not only uses the spectral decomposition method discussed in the previous paragraph but also applies tuning theory to identify the existence of thin beds in seismic data besides giving its thickness values. The basis of one study (Barnes, Fink & Laughlin, 2004), involves the use of wavelets. In his study, both Gabor and Morlet wavelets were used. The study proved an estimate of the bed thickness could be made by correlating

observed spectra with model spectra which also provides a useful measure of confidence. Although this study has achieved an improvement in the detection and classification of the thicknesses of thin beds, discovering hydrocarbons in thin sands is still an ongoing research.

### ***2.3.2 Direct Hydrocarbon Detection***

Direct hydrocarbon detection also involves analysing seismic data using spectral decomposition. In doing spectral decomposition, there are various methods implemented in research papers like Short windowed Fourier Transform, Morlet wavelet based wavelet transform and Matching Pursuit Decomposition (Miao et al., 2007).

A direct detection technique by making a comparison between compressional wave (P) and shear (SH) wave seismic data was documented. Lab studies have shown that P-wave velocities face a significant reduction in velocity when it comes in contact with reservoir sand which contains gas. At the same time, it is also learned that SH-wave velocities are only marginally affected. Therefore, the study uses the P-wave as a direct hydrocarbon indicator (DHI) without a corresponding SH-wave DHI. Meanwhile, a P-wave DHI occurring together with a SH-wave DHI means that the drop in velocities was caused by lithological changes and not the presence of a hydrocarbon (Ensley, 1985). While this study manages to prove the existence of gas directly from seismic data there is no mention on detection and delineation of oil.

One of the researches done on direct hydrocarbon detection from seismic data used another spectral decomposition method called instantaneous spectral analysis (ISA) and managed to prove that ISA consistently showed low frequency shadows under gas reservoirs which can be observed in the figure that follows this paragraph. The study also says that ISA has three other ways in helping with the detection of hydrocarbons. First, it shows an abnormally large attenuation in a thick or in a highly unconsolidated gas reservoir. Next proposed method for hydrocarbon detection using ISA is through the observation of the occurrence of frequency-dependent AVO. Finally, ISA also shows selective illumination at the “tuning” frequency which can be distinct for rocks saturated with brine or gas (Castagna et al., 2003). More research is needed on the three other ways by which the study has claimed ISA could be used for hydrocarbon detection. Apart from that, the present ISA method of relying on low

frequency shadows under gas reservoirs does not help to indicate where exactly the reservoir starts or is first detected. It is hoped from our study's direct detection method, this issue can be addressed.

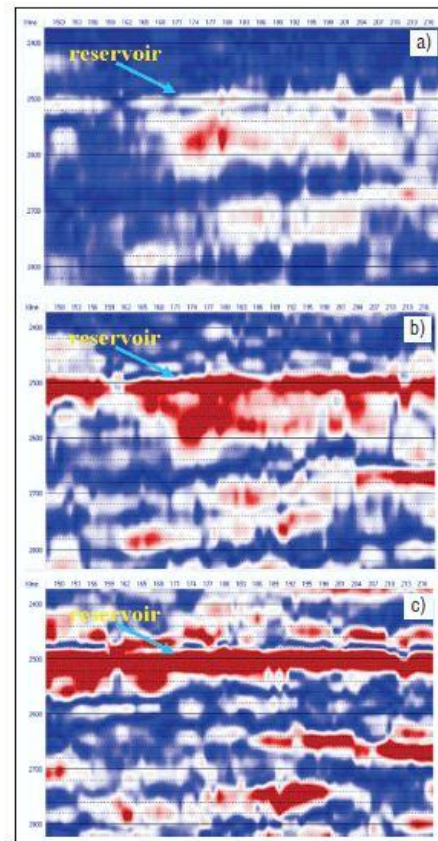


Figure 6: (a)8-Hz common frequency section. The low-frequency shadow just beneath the reservoir is the strongest event on the section (b) 12-Hz common frequency section. The low frequency shadow and the reservoir have comparable amplitude (c) 20-Hz section. The low frequency shadow is completely attenuated

Wavelet transform's potential in the use of direct hydrocarbon detection was explored by using tuning-related peak frequency that deviates from the norm in thin reservoirs. Just as previously applied in one of the studies for thin beds for indirect detection of hydrocarbons, Matching Pursuit Decomposition (MPD) method is used. Once the method is applied to the seismic trace, the difference in amplitude between lower frequency components to the higher frequency components is observed. It is also proven that the existence of low frequency shadows is an indicator of hydrocarbon reservoir in this method (Shengie & Castagna, 2002). However, performing many iterations of MPD is extremely expensive also takes up a lot of time (Barnes, Fink & Laughlin, 2004). Even though a reliable technique for direct detection of hydrocarbon

is needed, it should also be economically viable. Therefore, our study will aim to develop a technique that takes up a reasonable amount of time and cost.

The fractal analysis method called the Wavelet Transform Modulus Maxima Lines (WTMML) is also used in an attempt to detect hydrocarbons. The WTMMLs is able to produce singularity spectra that represent the various discontinuities present in the seismic data. The research has shown that the singularity spectra are affected by different lithology and different pore fluid types. Even more promising was the fact that these changes could be observed even though seismic amplitudes were not able to distinguish them.

The research done by Devi and Cohen (2004) has shown that it is possible to detect hydrocarbons using the WTMML method. Although the research mentions that singularity spectra that describe lithology can be easily differentiated from singularity spectra describing hydrocarbons, there was no further analysis on other spectral attributes of the singularity spectrum. Our study believes that there are more attributes of the singularity spectrum that can be analysed for the detection and delineation of hydrocarbons.

While there has been research in detecting hydrocarbons directly from seismic data, there is little mention on delineation process. Most studies have strictly focussed on gas. Our study aims to not only detect gas reservoirs, but also oil reservoirs from seismic data. Once the detection can be done, the study will also attempt to delineate the reservoir fluids by using fractal analysis and the singularity spectra that result from the process.

#### **2.4 Fractal Analysis using Wavelet Transform Modulus Maxima Method to compute the singularity spectrum**

The Wavelet Transform Modulus Maxima (WTMM) method is a well described method and a lot of research has been put into the betterment of the procedures involved. This study would also be using the WTMM method to generate the singularity spectra and in this section, all the steps will first be laid out. This section will also then describe each step a little further so the significance of each of these steps becomes clear to the reader.

The steps that need to be taken to compute the singularity spectrum are (Staal, 1995):

1. Perform continuous wavelet transform on the function  $f(t)$  where  $t$  is the time variable. The mathematical expression of the transform can be seen below,

$$W\{f, \psi\}(\sigma_0, \tau) = \int_{-\infty}^{+\infty} f(t) \frac{1}{\sqrt{|\sigma|}} \psi \left( \frac{t - \tau}{\sigma} \right) dt$$

2. Take the absolute value of the Wavelet Transform and find the local maxima as a function of position at each scale. A maxima point can be defined as follows:
  - A local extremum of  $W\{f, \psi\}(\sigma_0, \tau)$  is that point  $(\sigma_0, \tau_0)$  such that  $\frac{dW\{f, \psi\}(\sigma_0, \tau)}{d\tau}$  has a zero crossing at  $\tau = \tau_0$  when  $\tau$  varies.
  - A modulus maximum is any point  $(\sigma_0, \tau_0)$  such that  $|W\{f, \psi\}(\sigma_0, \tau)| < |W\{f, \psi\}(\sigma_0, \tau_0)|$  when  $\tau$  belongs to either the right or left of the neighbourhood of  $\tau_0$  and  $|W\{f, \psi\}(\sigma_0, \tau)| \leq |W\{f, \psi\}(\sigma_0, \tau_0)|$  when  $\tau_0$  belongs to the other neighbourhood of  $\tau_0$ .
3. Connect all points that are modulus maxima along the scale-time plane to obtain maxima lines
4. Track the maxima across scales. We track maxima lines for increasing scale  $\sigma$  by choosing at each scale the maximum between all previous values at smaller scales  $\sigma_0 < \sigma$ .
5. Compute the partition function  $Z(\sigma, q)$
6. Compute the scaling exponents  $\tau(q)$ . The slope of the log-log plots of  $Z(\sigma, q)$  versus  $\sigma$  by linear regression is computed to obtain  $\tau(q)$ . This can be represented mathematically as the equation below:

$$\tau(q) = \lim_{\sigma \rightarrow 0} \frac{\log Z(\sigma, q)}{\log \sigma}$$

7. Compute the singularity spectrum. By performing Legendre Transform on  $\tau(q)$  the values of the Holder exponents,  $\alpha$  and fractal dimensions,  $f(\alpha)$  can be obtained.

These steps mentioned above forms the fractal analysis approach that will be used in this study. The study will now attempt to explain each step so the reader could understand the underlying concept within these steps.

### 2.4.1 The Continuous Wavelet Transform (CWT)

Singular points or irregular points in a signal are points that undergo sudden changes that last for a short time. These abrupt changes in frequency cannot be analysed in detail by Fourier analysis as it only produces a spectrum of all the frequencies that exist in the signal and does not give any information on the exact time when the discontinuity occurs. Therefore, wavelet transforms which give both the frequency component as well as the time component of a signal becomes a very important analysis tool when it comes to detecting singularities.

In the WTMM method, continuous wavelet transform is applied. The continuous wavelet transform is described mathematically as the following (Polikar, 2006, Staal, 1995):

$$W\{f, \psi\}(\sigma, \tau) = \int_{-\infty}^{+\infty} f(t) \frac{1}{\sqrt{|\sigma|}} \psi \left( \frac{t - \tau}{\sigma} \right) dt$$

The equation above means that the transformed signal is a function of two variables, namely  $\tau$  and  $\sigma$  where the former is the translation parameter while the latter is the scale parameter. Scale here is the inverse of frequency thus that means lower scales represent higher frequencies while larger scales represent lower frequencies. The analysing wavelet is  $\psi(t)$ .

Once the analysing wavelet has been decided upon, continuous wavelet transform starts with the smallest value of  $\sigma$ . This means that the analysing wavelet will be in its most compressed state in. Taking the smallest scale to be  $\sigma = 1$  for instance, the analysing wavelet then starts its analysis of the signal from  $\tau = 0$  until the maximum value of  $\tau$ . What the analysing wavelet does is that it convolves with the analysing signal at every value of  $\tau$  for the scale of  $\sigma = 1$  and returns a value which represents the degree of similarity of the signal to the analysing wavelet at that scale which is termed as the coefficient of the wavelet transform. When this computation is done, the coefficients for the entire signal for the scale  $\sigma = 1$  will be obtained. Higher coefficient values correspond to a higher degree of similarity of the signal to the analysing wavelet and vice versa for lower coefficients. The process is then continued for all remaining scales.

The figures below show the CWT process in pictures:

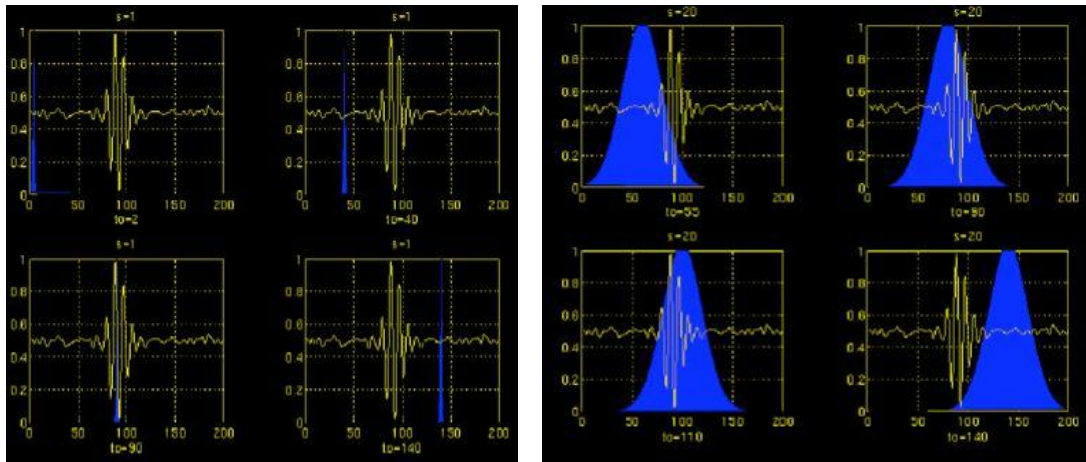


Figure 7: (a) Wavelet transform for scale  $\sigma=1$ . Figure shows the analysing wavelet (blue), narrow since it is at the lowest scale trying to capture high frequency components in the signal (yellow) that are similar to it (b) Wavelet transform repeated for scale  $\sigma=20$ . (Polikar,2006)

Once the CWT is completed on the signal being analysed, the results are plotted with scale occupying the y-axis and translation occupying the x-axis and finally the value of the coefficients taking the z-axis. However, typically CWT coefficients are described using colour plots as seen in the figure below. The figure below shows that the coefficients have a higher value at higher scales. This means that this signal contains more low frequency components rather than high frequency components.

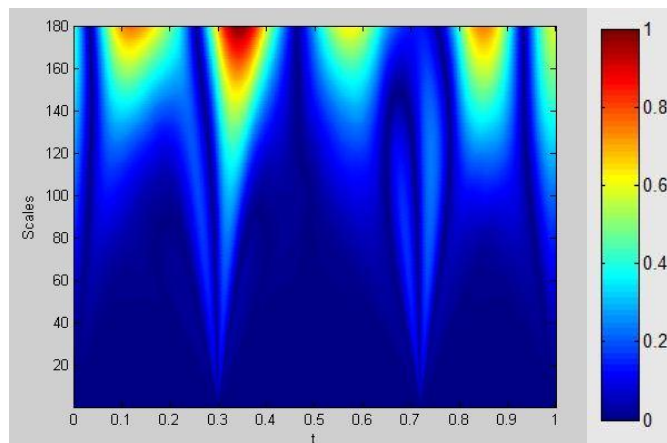


Figure 8: An example of the coefficients of the continuous wavelet transform pictured in colour form in FracLab with the legend denoting the coefficients' amplitude based on colours

#### 2.4.1.1 Finding Modulus Maxima Points

Once the continuous wavelet transform has been completed, the modulus of the coefficients is taken. The modulus maxima points can be identified as follows:

- A modulus maximum is any point  $(\sigma_0, \tau_0)$  such that  $|W\{f, \psi\}(\sigma_0, \tau)| < |W\{f, \psi\}(\sigma_0, \tau_0)|$  when  $\tau$  belongs to either the right or left of the neighbourhood of  $\tau_0$  and  $|W\{f, \psi\}(\sigma_0, \tau)| \leq |W\{f, \psi\}(\sigma_0, \tau_0)|$  when  $\tau_0$  belongs to the other neighbourhood of  $\tau_0$ .

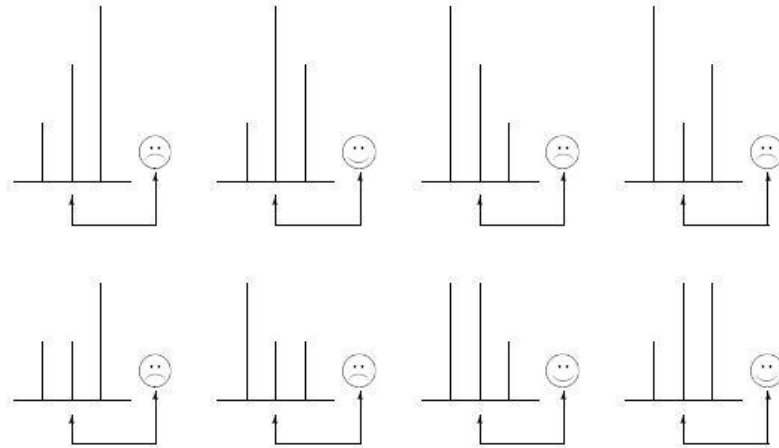


Figure 9: With reference to the points in the middle in all the pictures above, modulus maximum points are the points that have a happy smiley while the ones with the sad smiley are not modulus maxima points (Staal, 1995)

#### 2.4.1.2 Connecting Modulus Maxima Points to form Modulus Maxima Lines

The modulus maxima points found earlier are now connected from higher scales down to lower scales to form modulus maxima lines. A function cannot be said to be singular at a point  $t_0$  if there is no modulus maxima reaching down to the finer scales at that point. In other words, if there are modulus maxima points at the higher scales but none towards the finer scales, then there is no modulus maxima line, hence no singularity at that point in time. Therefore, it is important to keep in mind that although a singularity will cause a modulus maximum in the wavelet transform, a signal does not necessarily have singularities even if it has modulus maxima points in its wavelet transform (Mallat and Wen, 1992).

At this juncture it is important to mention that if a person only wishes to obtain the Holder exponent,  $\alpha$ , of the signal, then it can be done by finding the maximum slope of the lines that remain above the logarithm of the amplitude of the modulus maxima line, on a logarithmic scale (Staal, 1995).

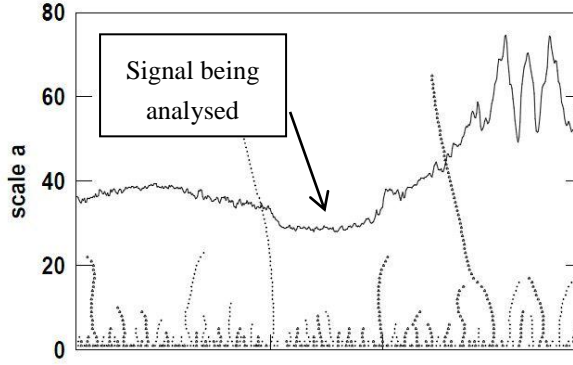


Figure 10: An example taken from Evertsz, Berkner & Berghorn (1995), showing modulus maxima lines in dotted lines for the signal which can be seen on the top half of the plot

### 2.4.2 Tracking maxima lines and computing partition function

As mentioned in the previous section on using WTMM lines to detect Holder exponents, this could be a task that would need a lot of computation time and resources especially if the signal contains a lot of WTMM lines. This is where using partition function can help to reduce the total computation needed. However, before dealing with the partition function, one other step that needs to be done is to track the maxima lines for increasing scale  $\sigma$  by choosing at each scale the maximum between all previous values at smaller scales  $\sigma_0 < \sigma$ . In other words, at the top of the maxima line, we will have the largest coefficient value in the entire length of the maxima line.

$$Z(\sigma, q) = \frac{1}{\sqrt{\sigma}} \sum_m (\sup \text{WTMML}(m))^q,$$

Where:

WTMML ( $m$ ) - is the  $m$ th wavelet transform modulus maxima line of  $W\{f, \psi\}(\sigma, \tau)$

$q$  - is the moment orders

$\sup$  - denotes the supremum of the WTMML( $m$ ) is to be taken

The reason for taking the supremum is to keep  $Z$  finite even when the amplitude of WTMML becomes small. This case arises when  $q < 0$  and the singularity is positive (Staal, 1995). This brings us back to why the maxima line was tracked in the previous step. This is to make it easier to obtain the supremum value of the WTMML ( $m$ ).

As mentioned earlier, the partition function helps to reduce computations as it is able to measure the scaling of moments and high order dependencies of wavelet coefficients and the singularity structure all in one. The moment order,  $q$ , is

responsible for detecting the singularities and represents the degree of polynomial (Khan, 2007). In simple terms, the analysing wavelet could be regarded as a box with its size being the scale,  $\sigma$ , while the modulus maxima lines then helps to indicate how to position these boxes to obtain a partition at the considered scale (Muzy, Bacry & Arneodo, 1993).

### 2.4.3 Computing scaling exponent, $\tau(q)$

Scaling exponent,  $\tau(q)$  is responsible for describing the statistical moments and it is related to the partition function  $Z(\sigma, q)$  in this manner (Muzy, Bacry & Arneodo, 1993):

$$Z(\sigma, q) \sim \sigma^{\tau(q)}, \quad \sigma \downarrow 0.$$

A plot of  $\log$  of  $Z(\sigma, q)$  versus  $\log$  of  $\sigma$  is plotted and the gradient for each value of  $q$  is taken to give the scaling exponents since:

$$\tau(q) = \lim_{\sigma \rightarrow 0} \frac{\log Z(\sigma, q)}{\log \sigma}$$

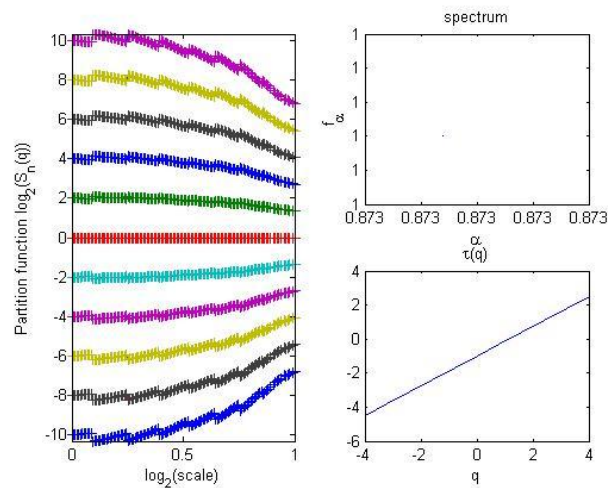


Figure 11: Partition function plot for different values of  $q$  seen on the left. The bottom right plot shows the scaling exponent plot for a sine wave in FracLab. The top right corner is the singularity spectrum generated

As will be explained in the following step, the values of Holder exponents,  $\alpha$  and fractal dimensions,  $f(\alpha)$  can be extracted.

#### 2.4.4 Compute singularity spectrum using Legendre Transform

It is common practice to relate two parameters, an independent variable and a dependent value using a function like  $f(x)$  where  $x$  is the independent variable while  $f$  is the dependent variable. There are times when there is a need to describe the same function in a more convenient way. This is the function of Legendre Transform. However,  $f(x)$  must meet two very important conditions (Zia, Redish & McKay, 2007):

- i.  $f(x)$  must be convex and is smooth. What this means is that the second derivative of  $f(x)$  does not change sign while being smooth means it has to be continuously differentiable to a certain extent.
- ii. It must be easier to obtain data from the derivative of  $f(x)$  than to use  $x$  itself.

Since the scaling exponent,  $\tau(q)$  contains the values of Holder exponents,  $\alpha$  and fractal dimensions,  $f(\alpha)$ , by performing Legendre Transform to it, this information can be obtained. The relation between  $\tau(q)$ ,  $\alpha$  and  $f(\alpha)$  can be seen as follows (Staal, 1995):

$$\frac{d\tau(q)}{dq} = \alpha \quad f(\alpha) = q\alpha - \tau(q)$$

Looking at these equations above,  $q$  is actually just the slope of  $f(\alpha)$  since:

$$\frac{df(\alpha)}{d\alpha} = q$$

This means that, in the partition function  $Z(\sigma, q)$ , each  $q$  used will give one value of Holder exponent,  $\alpha$  in the singularity spectrum. To understand this statement, a singularity spectrum that was generated for a sine wave signal is shown below and an explanation follows after the figure.

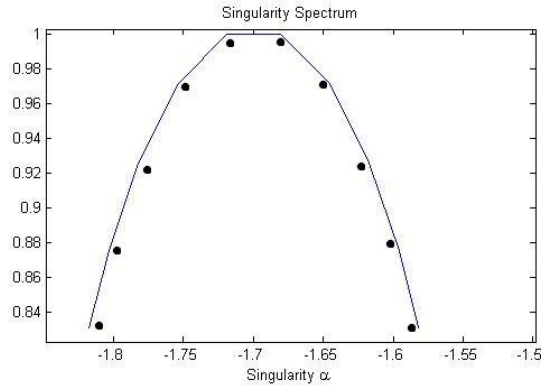


Figure 12: An example of a singularity spectrum produced on FracLab. The dots have been added to show where the gradient,  $q$  which is also the mass exponent changes

The above singularity spectrum shows what was meant when we say that each  $q$  represents one value on the singularity spectrum. Looking at the spectrum above, the different gradients can be seen at those points highlighted with a dot. As we know  $q$  is the gradient of the singularity spectrum. Thus the more number of moment orders,  $q$ , used in doing the partition function, the more number of Holder exponents can be detected. Also, this means that positive  $q$  values will reside on the left side of the peak of the singularity spectrum while negative  $q$  values will reside on the right side of the curve with  $q = 0$  being the point at the peak of the curve.

Apart from that, it is important to note that the singularity spectrum is actually a probability distribution of Holder exponents,  $\alpha$  with fractal dimensions,  $f(\alpha)$  being the probability of occurrence of a particular  $\alpha$  (Khan, 2007). Some points can be derived from this as well as we can see below (Makowiec, Rynkiewicz, Galaska, Wdowczyk-Szulc & Zarczynska-Buchowiecka, 2011):

- The  $\alpha$  points on the left extremity and right extremity of the singularity spectrum are the least occurring singularities in the signal that is analysed.
- The  $\alpha$  on the left extremity of the singularity spectrum points to the strongest singularity in the signal being analysed while the  $\alpha$  on the right extremity of the singularity spectrum points to the weakest singularity in the signal.
- For a  $\alpha$  that has a fractal dimension,  $f(\alpha) = 1$ , that means that the signal being analysed contains that singularity the most.

Going back to the scaling exponent,  $\tau(q)$ , if it produces a straight line like in Figure 11, it is bound to have only one gradient, which means it will have only one  $\alpha$  value. This means that the function that is being analysed is a monofractal signal since it only has one type of singularity (Faghfouri and Kinsner, 2005). Meanwhile, a multifractal signal is one that produces a singularity spectrum with more than one point. For multifractal signals, the  $\tau(q)$  will be a curve with more than one gradient (Faghfouri and Kinsner, 2005).

## CHAPTER 3

### RESEARCH METHODOLOGY

#### 3.1 Project Activities

The study will be divided into two phases. The first phase of the study will be focused on the first objective and it will be done during the first semester of my final year. Meanwhile, in the second phase of the study, the second objective, that is to come up with a direct detection method for hydrocarbon detection will be done.

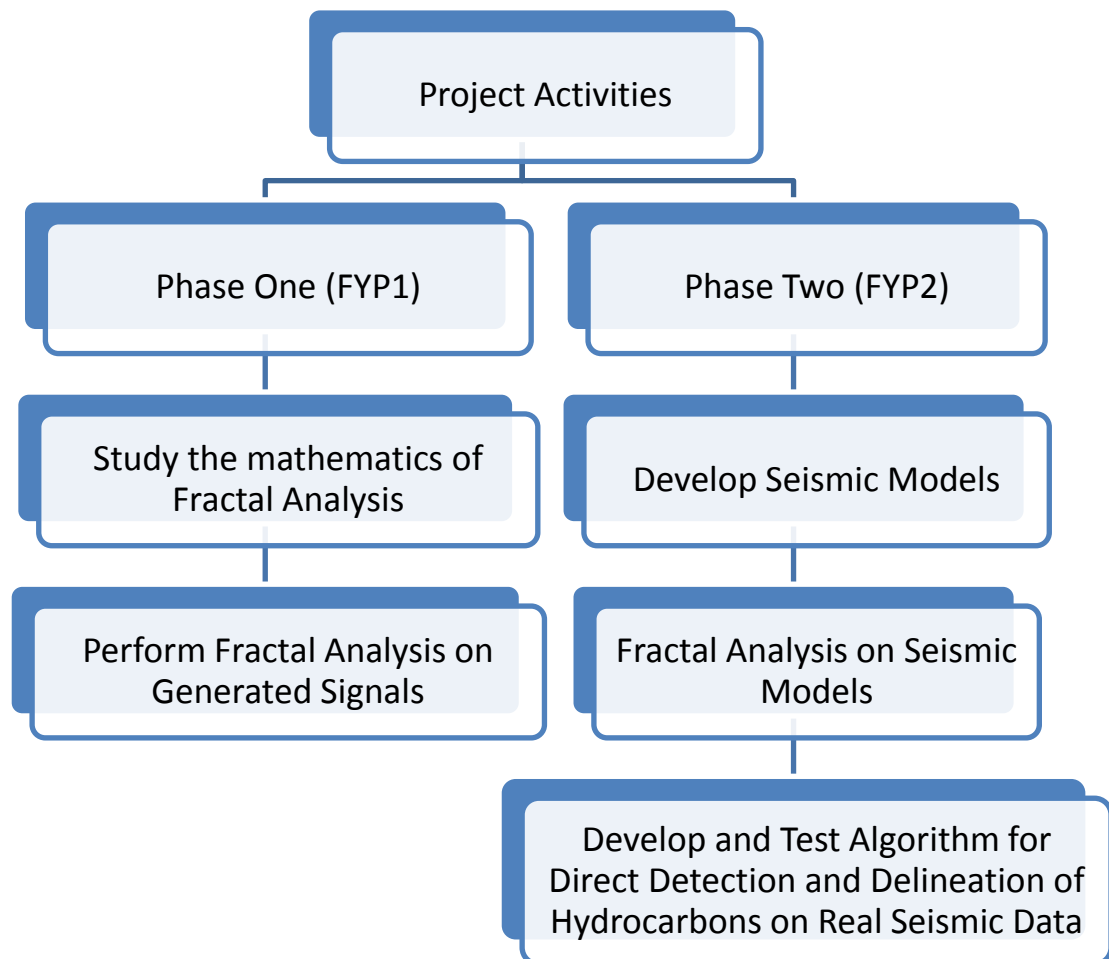


Figure 13: Flowchart of research methodology

### **3.1.1 PHASE ONE – FYPI**

#### **1) Developing a clear understanding of the mathematics behind fractal analysis**

Fractal analysis is a collection of mathematical steps that have to be carried out in order to obtain the singularity spectrum. The fractal analysis method used in this study is the Wavelet Transform Modulus Maxima (WTMM) method. The steps involved have been discussed in length in the literature review section. There are some extensive literature on fractal analysis like the work of Staal (1995) and Faghfour and Kinsner (2005). The steps undertaken to understand the mathematics of fractal analysis was to read these literature sources and clear any doubts that came up by meeting Dr. Ibrahima Faye.

#### **2) Perform Fractal Analysis on Various Signals**

To do this, the FracLab toolbox is used. Different signals are generated using MATLAB and their singularity spectra are generated using FracLab. These signals are changed in various ways, like amplitude, number of cycles of a certain signal, type of signal (square wave, triangular wave) among others. Their effects on the singularity spectrum are observed and the study will try to categorize singularities and their degree of irregularity based on the response seen in the singularity spectrum. The study will also try to see if these changes agree with the mathematics that has been discussed previously.

As mentioned in the earlier sections of this paper, this study would be using the Wavelet Transform Modulus Maxima (WTMM) method as the fractal analysis method to generate the singularity spectrum. FracLab provides this method under its multifractal spectra tab.

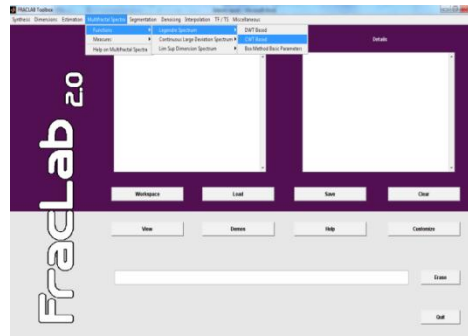


Figure 14: Snapshot of Fraclab toolbox

The steps involved in obtaining the singularity spectrum using Fraclab are as follows:

1. The signal – given the variable  $y$  for instance - that we intend to analyse is first generated in MATLAB.
2. The variable,  $y$  is then imported into Fraclab.
3. In order to perform fractal analysis using WTMM method, the following option is used.
  - Multifractal Spectra >> Functions >> Legendre Spectrum >> CWT Based.

This means that by using Continuous Wavelet Transform (CWT) and the Legendre Spectrum, the singularity spectrum is generated.
4. Select between using Basic and Advance parameters. Before the singularity spectrum is generated, we have to first select between Basic and Advanced parameters. Since at the moment only analysis of test signals are done, basic parameters will suffice to describe any pattern that arises from analysing the different type of signals.
5. Singularity spectrum is generated.

### 3.1.2 PHASE 2 – FYP 2

#### 1) Development of seismic models

A possible application of fractal analysis that this research is interested on is the possibility of detection of hydrocarbons directly from seismic data. At present, seismic data is used together with other well log data like gamma ray and resistivity data to predict the possible location of hydrocarbon reservoirs. Now, with the ability of fractal analysis to characterize different irregular signals via the singularity

spectrum, the idea of using seismic data alone to detect hydrocarbons can be explored.

This study first conducted tests on seismic models. Seismic data is generated by collecting the sound waves that is reflected from the various layers under the earth's surface. Therefore seismic data is essentially a collection of irregular signals. Seismic data is a representation of the acoustic properties of the layers found beneath the surface. The acoustic property of each layer is governed by its density and velocity. The density and velocity of the layers changes from one layer to the next. The location where this change occurs is where the reflection of the sound waves takes place.

With this knowledge the seismic models were generated. The steps behind generating a seismic model can be seen as below:

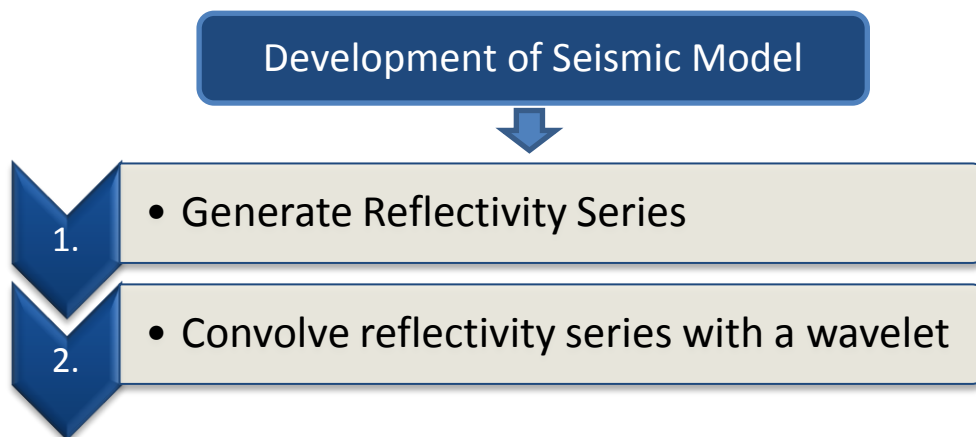


Figure 15: Steps to develop seismic models

### 1. Generating reflectivity series

Each layer within the earth has its own acoustic impedance. Acoustic impedance, usually symbolized by  $Z$ , can be defined as the product of density and seismic velocity, and these two properties are not the same for different rock layers. It is this change in acoustic impedance between layers that cause the seismic wave to be reflected back to the receivers on the surface. This reflected sound wave is seen as a reflection coefficient. The reflection coefficient tells us how much energy is reflected. A collection of these reflection coefficients makes up a reflectivity series.

The reflection coefficient can be expressed by the following equation:

$$R = \frac{\rho_2 V_2 - \rho_1 V_1}{\rho_2 V_2 + \rho_1 V_1}$$

where  $R$ = reflection coefficient  
 $\rho_2$ = density of medium 2  
 $\rho_1$ = density of medium 1  
 $V_2$ = velocity of medium 2  
 $V_1$ = velocity of medium 1

In this study, the density and velocity used for each medium can be seen as follows:

Table 1: Density, Velocity and Acoustic Impedance of different subsurface layers (Khan, 2007)

Subsurface Layers	Velocity (km/sec)	Density (gm/cc)	Acoustic Impedance (gm.km/sec.cc)
Gas Sand	2.479	1.833	4.544007
Oil Sand	2.809	2.147	6.030923
Wet Sand	2.934	2.180	6.39612
Shale	2.94	2.38	6.9972

With these values, the reflectivity series can be generated based on our own parameters for thickness of each layer and the type of layers in the model. It is important to note that when setting the thickness of each layer, the layer's own velocity value must be taken into consideration. Also, the fact that the sound wave travels two ways – both downwards then reflected back upwards - within each layer before reaching the surface must also be taken into account. In general, the time to depth conversion is as following:

$$d = \frac{Vt}{2}$$

Where  $d$  = depth

$V$  = velocity

$t$  = time taken for reflection to reach the surface

Adapting the formula above, the thickness of each layer can also be set according to our preference provided the right velocity value is used for each layer.

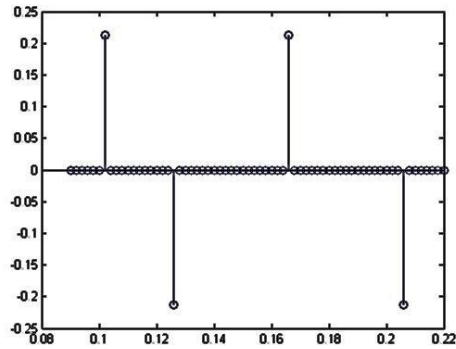


Figure 16: An example of the reflectivity series produced

In generating these seismic models, there are two assumptions made. The first assumption is that the density and velocity values of the layers do not change with change in depth. Second, the reflected signal is not affected by energy loss i.e. the amplitude of the reflection coefficients are the same if the interface between subsurface layers where the reflection occurs are the same, regardless of depth.

## 2. Convolve Reflectivity Series with a wavelet

The next step is to convolve the reflectivity series with a suitable wavelet. One of the most commonly used wavelets convolved with the reflectivity series to generate a synthetic seismogram is the Ricker wavelet. The Ricker wavelet is a zero phase wavelet.

A key factor when it comes to Ricker wavelet is selecting its centre frequency. Wavelets used in the field are generally of lower frequencies. The reason for this is because the wavelets lose its energy with time in the form of heat during propagation. The energy loss is significant especially when the wavelet used is of high frequencies. Therefore, in line with real life seismic application, the study uses a Ricker wavelet with a centre frequency of 60Hz.

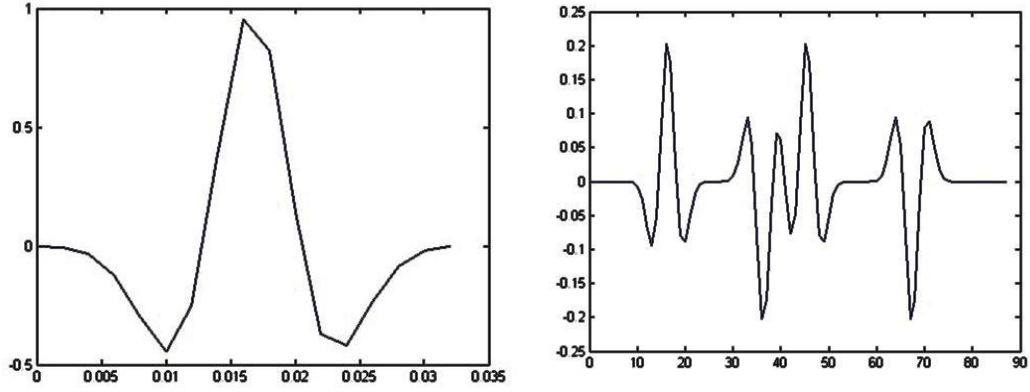


Figure 17: (a) Ricker wavelet with 60Hz centre frequency (b) Reflectivity series after convolved with ricker wavelet

## 2) Fractal Analysis on the Seismic Models

Next, fractal analysis was carried on the seismic models. This is to obtain the singularity spectra so as to be able to study the response of the singularity spectrum to different reservoir fluids. The two steps involved are mentioned below:

### i. Generate singularity spectrum by performing fractal analysis

Using the FracLab toolbox in MATLAB, singularity spectra are generated for each of the models using the same fractal analysis steps discussed previously. The choice of wavelet and other parameters used in the fractal analysis process is discussed in the results and analysis section of the study.

### ii. Analyse the results

From the singularity spectra generated in the previous step, various features of the singularity spectrum like the  $\alpha_{\text{peak}}$  value, width and asymmetry.  $\alpha_{\text{peak}}$  is the value of the Holder exponent that occurs the most in the signal under analysis. It means that the signal is mostly described by this particular singularity. Meanwhile, width and asymmetry is described by the equations below:

$$\text{Width} = \alpha_{\text{max}} - \alpha_{\text{min}} \qquad \text{Asymmetry} = \frac{\alpha_{\text{peak}} - \alpha_{\text{min}}}{\alpha_{\text{max}} - \alpha_{\text{peak}}}$$

Width of the singularity spectrum tells us how widely spread the singularities are in a signal. Finally, asymmetry values above 1 show that the signal is described by

singularities that are more irregular than the  $\alpha_{\text{peak}}$  value and vice versa for values below 1.

### 3) Develop and test algorithm for direct detection and delineation of hydrocarbons on real seismic data

In order to develop an algorithm for direct detection of hydrocarbon, real seismic data from a wild cat well was obtained. The data obtained is essential for the progression of this study as actual seismic data is needed for the development of a reliable direct hydrocarbon detection and delineation algorithm. Using fractal analysis as the basis, an algorithm for direct detection of hydrocarbons was developed. The following are the steps involved in the algorithm:

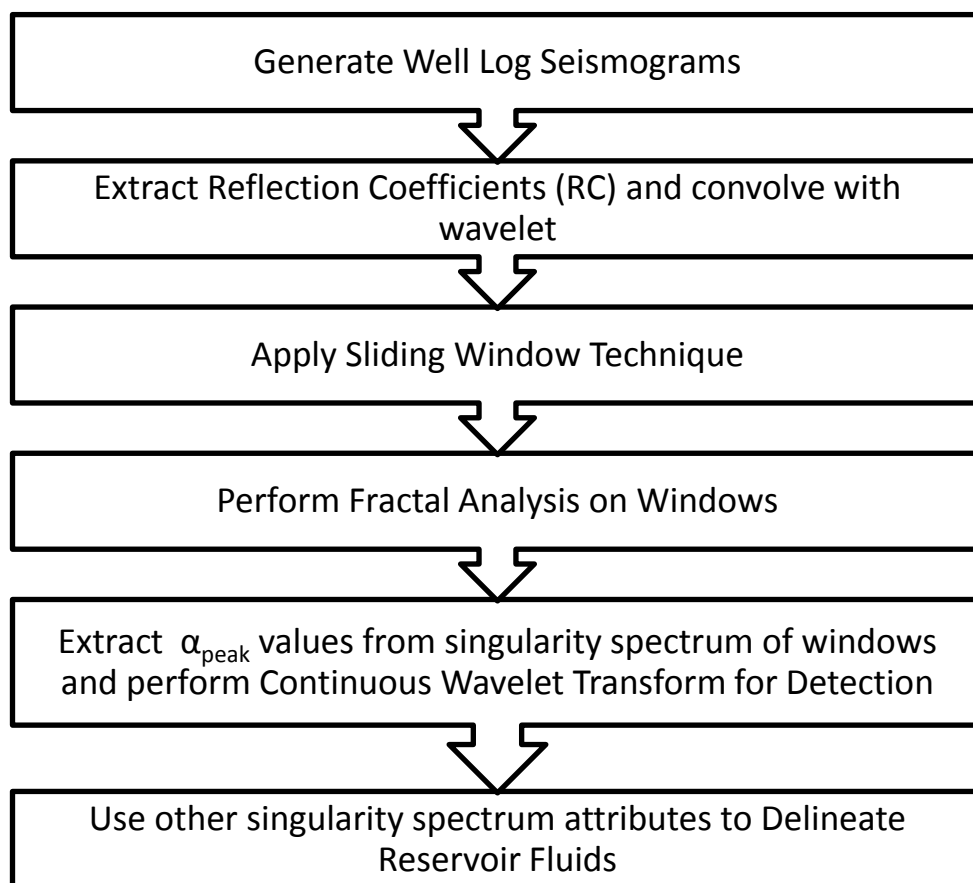


Figure 18: Flowchart of the steps involved in the Direct Detection and Delineation Algorithm

**i. Develop Well Log Seismograms**

From the raw seismic data, a well log Seismogram was generated using the software Petrel. The seismogram that is generated for the well under study can be seen in the following figure. The seismogram is produced with the sonic logs and density logs that were available.

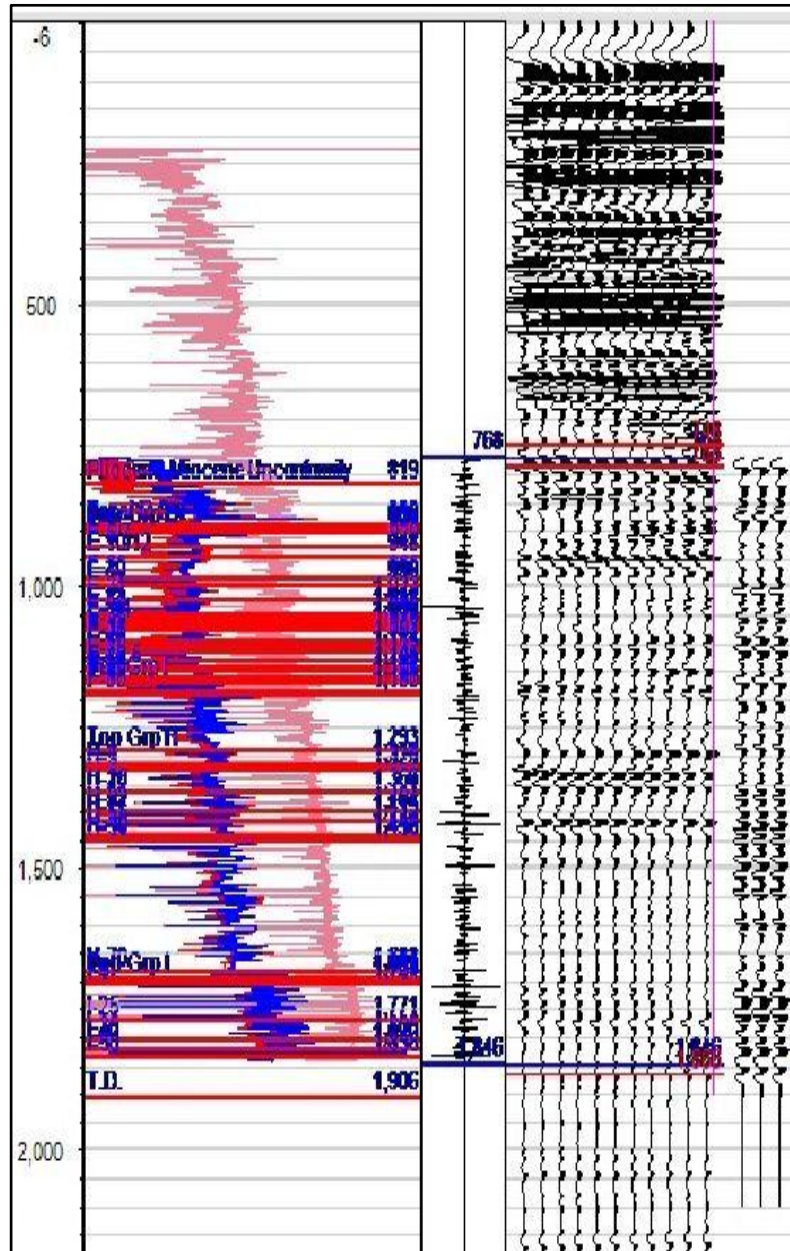


Figure 19: Synthetic seismogram of the well

**ii. Extract reflection coefficients and convolve with wavelet**

From the well log seismogram, Petrel calculates the reflection coefficients values. Just as previously seen with the seismic modelling, the reflection coefficients must be convolved with a wavelet. The choice of wavelet has to be a low frequency wavelet as used in the field. Therefore, a Ricker wavelet with a center frequency of 60Hz is used in this study to produce the seismic trace in MATLAB.

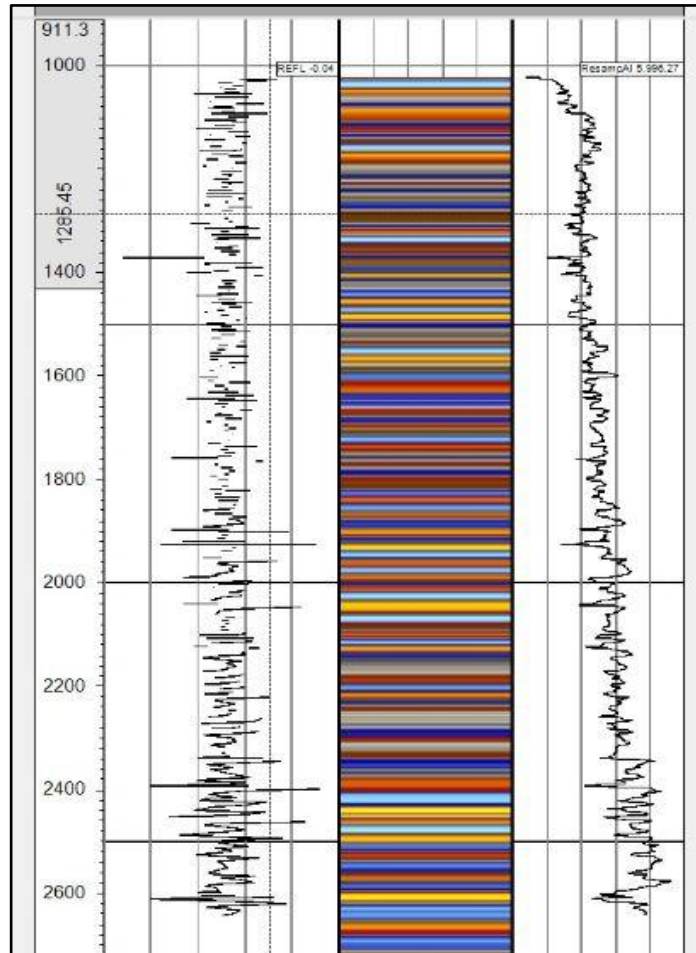


Figure 20: Reflection coefficient and acoustic impedance

**iii. Apply sliding window technique**

The windowing technique is obtained from the work of Khan (2007) and adapted to suit this study. The reflection coefficients are partitioned into numerous signal segments or windows. Two crucial factors in applying the windowing technique is:

**a. Optimum Window Length**

- This controls the depth of analysis of each window

b. Window Displacement

- In relation to the seismic trace, window displacement is an indication of how many samples are covered each time the window is moved.

As explained by Khan (2007), in order to obtain a singularity spectrum from the samples in each window, a sufficient number of samples are required in every window. Therefore, the seismic trace was upsampled. The upsampling is done in MATLAB and a brief explanation can be seen as follows.

The upsampling of a signal with an integer factor,  $L$  will result in the sampling period changing from  $T$  to  $T/L$ . This is performed by inserting  $(L-1)$  zeroes between each sample in the original signal. Then the upsampled signal goes through a low pass filter. The combination of the upsampler and the low pass filter is known as the interpolator (Mohamad Hani, 1999). The figure below is the graphical representation of the steps:

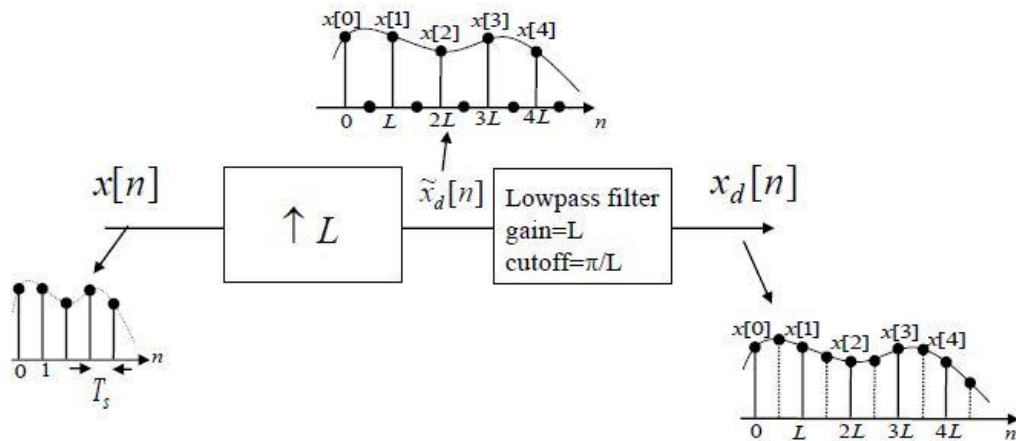


Figure 21: Upsampling process (Mohamad Hani, 1999)

The seismic trace was upsampled by a factor of 20 and each window contains two samples from the original signal. This means each window comprises of 40 samples. Since the seismic data from this well was sampled at 0.004s and the relative distance between each sample in terms of depth was approximately 1.5m, the depth of analysis per window is approximately 3m.

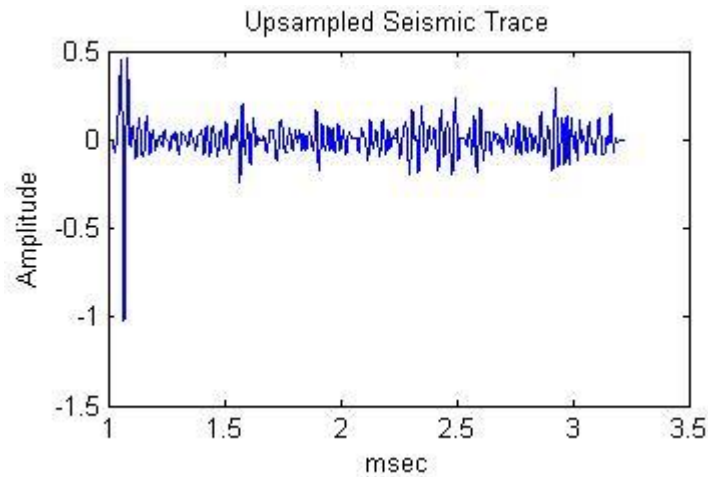


Figure 22: Upsampled seismic trace

#### iv. Perform Fractal Analysis on Windows

After the seismic trace is partitioned into windows, fractal analysis is performed on each window using the FracLab toolbox. The ‘Morlet – analytic’ wavelet is chosen as the analysing wavelet in this study.

The Morlet wavelet is a complex wavelet with no order or vanishing moment defined unlike the wavelets derived from the derivative of the Gaussian function. Choosing the Mexican Hat wavelet– which is the second derivative of the Gaussian function – for instance means that only singularities with  $\alpha$  values from negative infinity to +2 can be detected. Meanwhile, using the Morlet wavelet means this issue is dealt with since it does not have vanishing moments and can detect a broader range of  $\alpha$  value. This is suitable for this study since we do not know the range of singularities that are found in the seismic data beforehand.

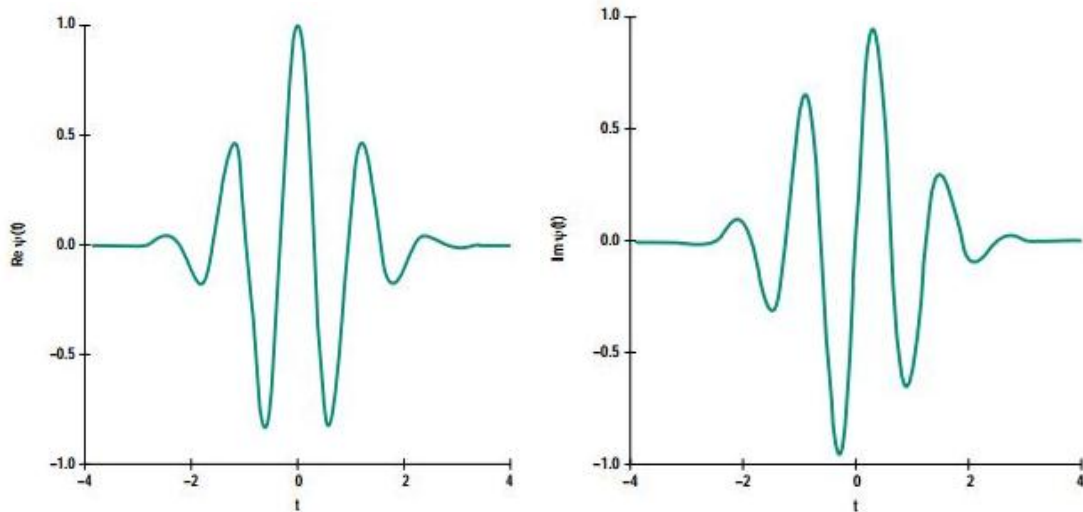


Figure 23: (a) Real part of the Morlet wavelet (b) Imaginary part of the Morlet wavelet

**v. Extract  $\alpha$  peak values from singularity spectrum of windows and perform Continuous Wavelet Transform for Detection**

The singularity spectrum attribute that is used for detection of hydrocarbon is the  $\alpha_{\text{peak}}$  values.  $\alpha_{\text{peak}}$  is the value of the singularity that occurs most in the signal being analysed. The  $\alpha_{\text{peak}}$  value obtained from each window is plotted and continuous wavelet transform is performed on this plot. The results and analysis section will explain further on what is expected from the continuous wavelet transform for the detection of hydrocarbons.

**vi. Use other singularity spectrum attributes to Delineate Reservoir Fluids**

Once the windows with high energy have been identified from the continuous wavelet transform in the previous step, other singularity spectrum attributes like width and asymmetry are used together with the  $\alpha_{\text{peak}}$  values to delineate the reservoir fluid in these regions. The results of the delineation process i.e. the analysis of the width, asymmetry and  $\alpha$  peak are compared to the well report to identify if indeed the regions contain gas or oil.

## 3.2 Tools and Software Required

Software required:

- **FracLab toolbox in MATLAB**

FracLab was developed for free by the Regularity team at Inria Saclay/Ecole Centrale de Paris as a tool that performs general purpose signal and image processing through fractal and multifractal methods. The software provides the user with various fractal tools to study irregular signals.

- **2. Petrel**

Petrel is a Schlumberger owned software that helps increase reservoir performance by improving asset team productivity. In this project, it was used to develop synthetic seismograms.

### 3.3 Gantt Chart and Key Milestones

Project Activities	Weeks in Semester 2															
	S* 1	1	2	3	4	5	6	7	8	9	10	11	12	13	14	15
Developing a clear understanding of the mathematics behind fractal analysis - Reading various literature sources - Meet mathematics lecturer to clear doubts																
Fractal analysis on various signals - Analyse effects of change on signal towards singularity spectrums																
Development of Seismic Models - Read various related literature - Develop actual seismic models					M1*											
Fractal analysis on seismic models - Generate singularity spectrums - Analyse the singularity spectrums							M2*									
Progress Report - Preparation and submission of progress report									M3*							
Development of Algorithm for direct detection of hydrocarbon - Obtain real seismic data from PETRONAS - Create the algorithm in MATLAB													M4*			
Final Report - Preparation and submission of draft report - Submission of final report															M5*	
VIVA																

\*S1 – Semester 1 / FYP 1

\*M1 – Milestone 1 – Successful development of seismic models

\*M2 – Milestone 2 – Singularity spectrums for different seismic models generated and analysed

\*M3 – Milestone 3 – Submission of progress report

\*M4 – Milestone 4 – Development of direct detection algorithm

\*M5 – Milestone 5 – Submission of Final Report

# CHAPTER 4

## RESULTS AND ANALYSIS

### 4.1 Results and analysis of singularity spectrum for various signals

#### 4.1.1 Type of signals

In this test, three types of signals, sine waves, sawtooth waves as well as square waves are tested. All other variables like sampling rate and number of periods for each type of wave are kept the same.

- Sine wave – **Sampling rate =  $10 \cdot f_0$ . Period = 1. Amplitude = 1**

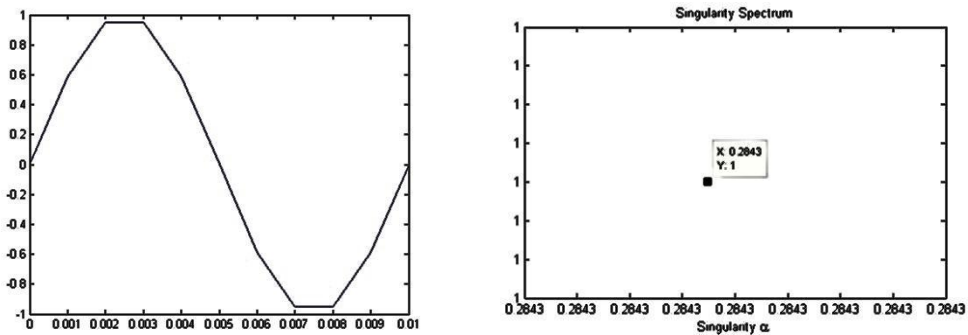


Figure 24: (a) The sine wave used for this test, (b) Singularity spectrum produced for the sine wave

- Sawtooth wave – **Sampling rate =  $10 \cdot f_0$ . Period = 1. Amplitude = 1**

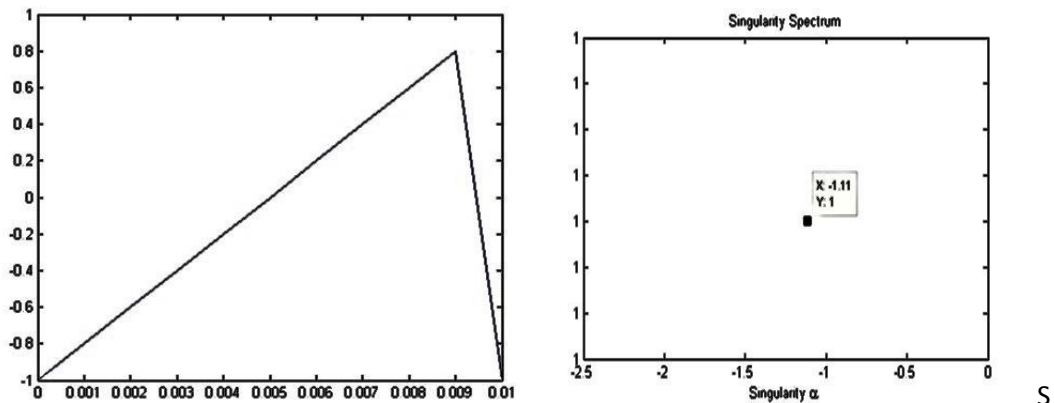


Figure 25: (a) Sawtooth wave used for this test, (b) Singularity spectrum produced for the sawtooth

- Square wave – **Sampling rate** =  $10 \cdot f_0$ . **Period** = 1. **Amplitude** = 1

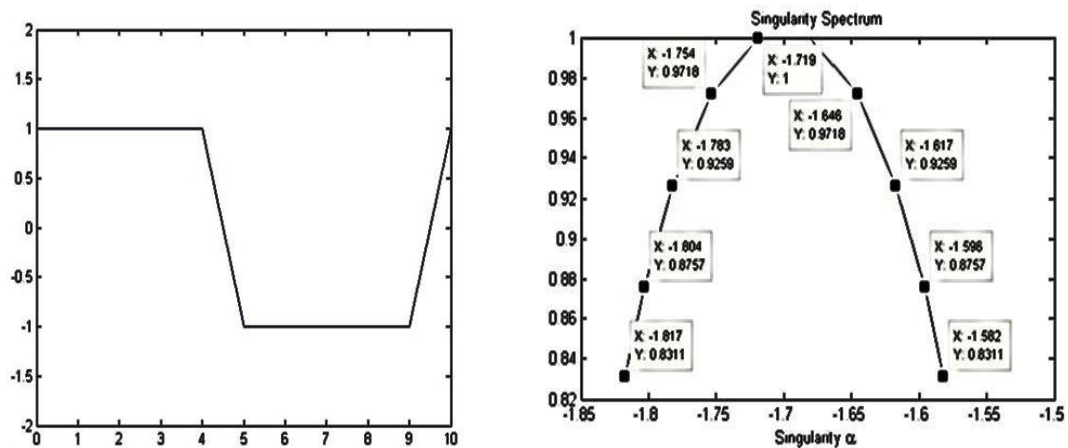


Figure 26: (a) Square wave used for this test (b) Singularity spectrum produced for the square wave

First looking at the results produced by the sine wave, only a dot is produced. This means that only one type of singularity exists in the signal, which is what is expected of a sine wave since it is a smooth wave made up of just one frequency component. Moving on to the sawtooth wave, its singularity spectrum also reveals that the signal only has one type of singularity. This is the expected result since in essence a singularity spectrum gives an  $\alpha$  value for all singularities present in a signal. In the sawtooth wave only one singularity is present, which is when the amplitude drops from 1 to 0. Finally, the square wave produced a spectrum of points rather than a single point indicating that more than one singularity exists within the signal. The square wave has more than one transient and these transients are reflected by the  $\alpha$  values in the singularity spectrum.

When comparing the three signals together, we look at the values of  $x$  (Holder exponent,  $\alpha$ ) on the singularity spectrum. This is because a smaller Holder exponent value means that the signal is more irregular. As expected the sawtooth wave has a smaller value for its Holder exponent ( $\alpha = -1.11$ ) compared to the sine wave since ( $\alpha = -0.2843$ ) it is more irregular than the sine wave. When comparing the singularity spectrum of the square wave to the other signals, the left most point ( $\alpha = -1.817$ ) – the strongest singularity - on the spectrum is taken as the comparison point. Since the square wave has more transients, the strongest singularity should be seen in the square wave and this is depicted by its singularity spectrum. Therefore, the results show that the square wave is more irregular than both sawtooth and sine waves.

### 4.1.2 Amplitude

- 1) Sine wave –**Sampling rate** =  $10 \cdot f_0$ . **Amplitude** = 0.1, 1 and 10. **Period** = 1

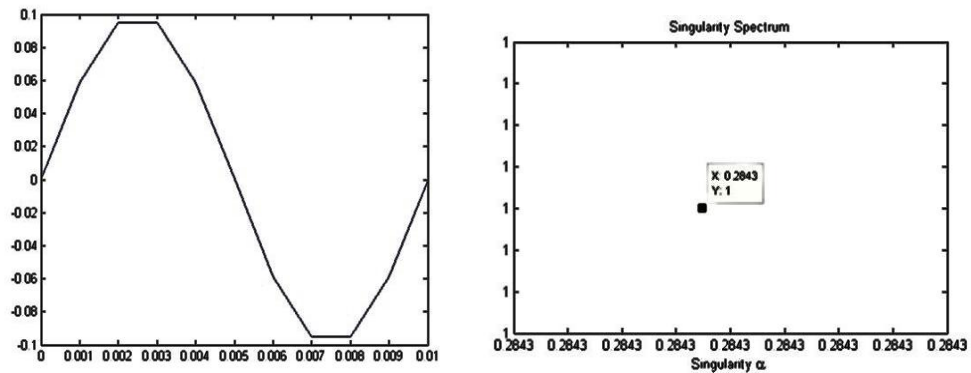


Figure 27: (a) One of the sine waves used for this test (amplitude = 0.1) (b) Singularity spectrum produced was a dot and it was the same for all different amplitudes of the sine wave

- 2) Sawtooth wave –**Sampling rate** =  $10 \cdot f_0$ . **Amplitude** = 0.1, 1 and 10. **Period** = 1

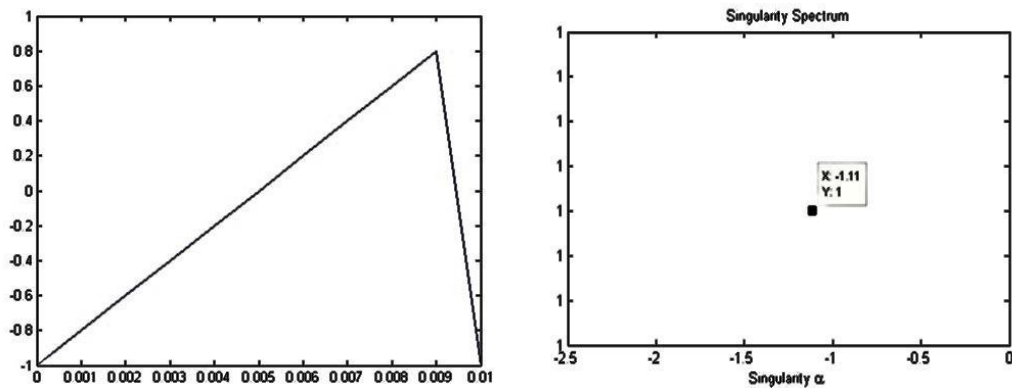


Figure 28: (a) One of the sawtooth waves used for this test (amplitude = 1), (b) Singularity spectrum produced was the same for all different amplitudes of the sawtooth signal

- 3) Square wave –**Sampling rate** =  $10 \cdot f_0$  **Amplitude** = 0.1, 1 and 10 **Period** = 1

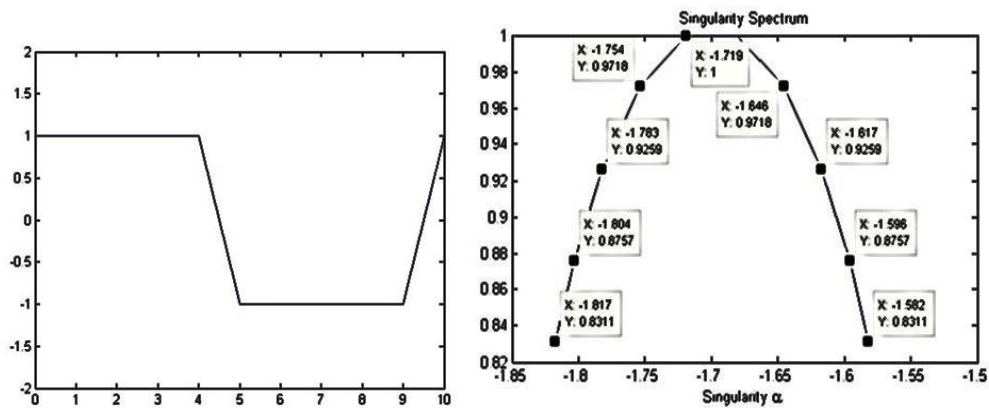


Figure 29: (a) One of the square waves used for this test (amplitude = 1), (b) Singularity spectrum produced was the same for all different amplitudes of the square waves

This time for each type of wave, only the amplitude was varied. The basis of fractal analysis is wavelet transform which is a mathematical analysis tool to detect transients or a rapid fluctuation in frequency. Therefore, it is expected that a change in amplitude should not affect the outcome of the singularity spectrum. Indeed for all three waves (sine wave, sawtooth and square wave it can be observed that even when the amplitude was changed from 0.1 to 1 and finally to 10, the singularity spectrum produced in each case was the same. This means the hypothesis that the singularity or singularities found within a signal does not change with a change in amplitude holds.

#### 4.1.3 Adding noise in the form of triangular pulse to the signal

1) Sine wave: **Sampling rate** =  $10 \cdot f_0$ . **Amplitude** = 1. **Cycle(s)** = 1

**Noise added** = Triangular pulse repeated every 0.002s within the total time of one sine cycle of 0.01 seconds

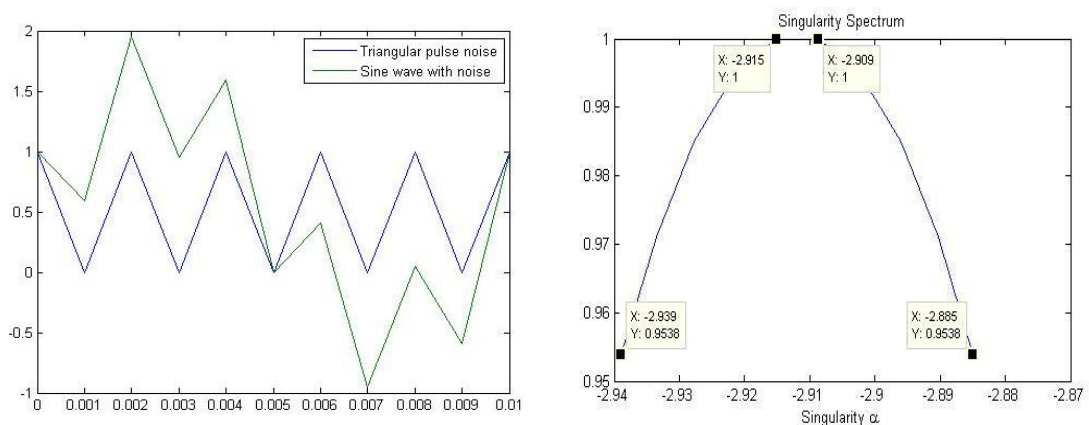


Figure 30: (a) The green signal is the sine wave after noise (blue) is added to it, (b) Singularity spectrum produced for the signal in (a)

2) Sine wave: **Sampling rate** =  $10 \cdot f_0$ . **Amplitude** = 1. **Cycle(s)** = 1

**Noise added** = Triangular pulse repeated every 0.003 seconds within the total time of one sine cycle of 0.01 seconds

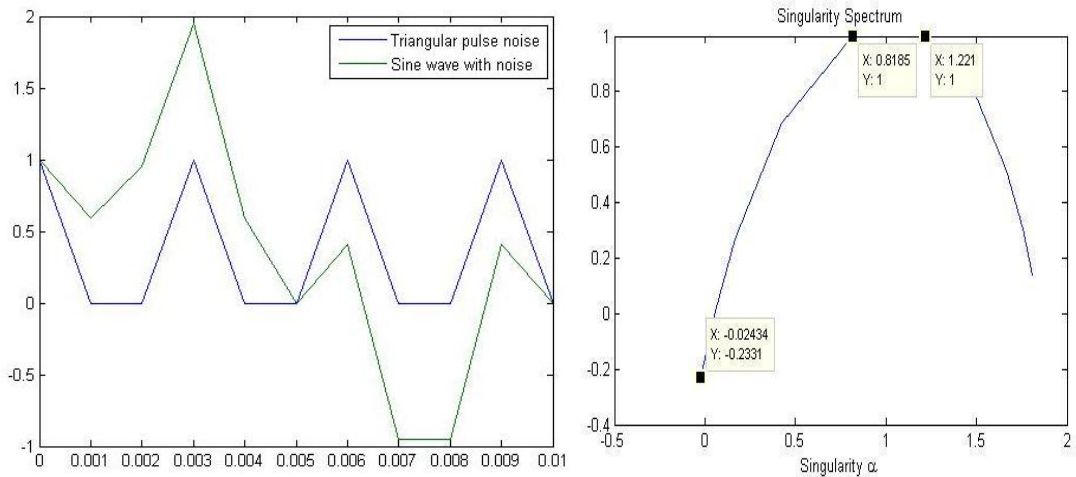


Figure 31: (a) The green signal is the sine wave after noise (blue) is added to it, (b) Singularity spectrum produced for the signal in (a)

3) Sine wave: **Sampling rate** =  $10 \cdot f_0$ . **Amplitude** = 1. **Cycle(s)** = 1  
**Noise added** = Triangular pulse repeated every 0.004 seconds within the total time of one sine cycle of 0.01 seconds

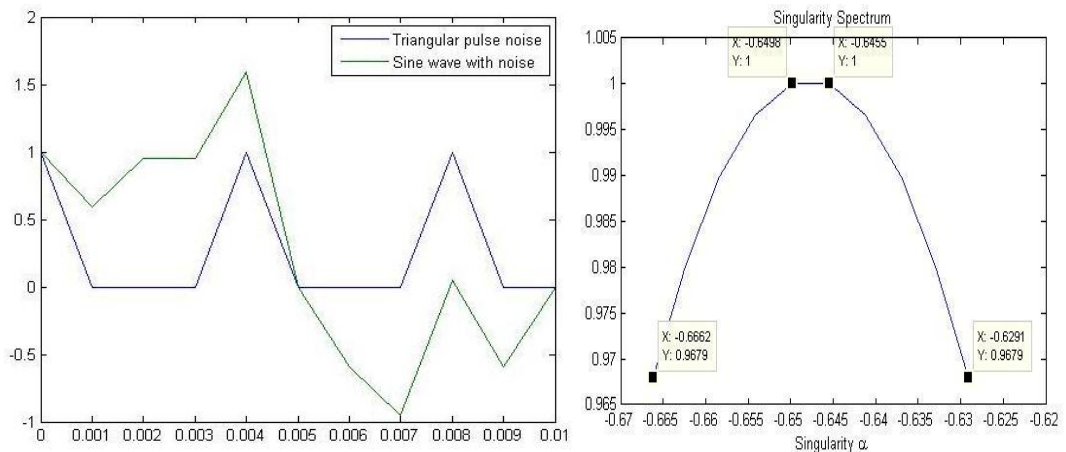


Figure 32: (a) The green signal is the sine wave after noise (blue) is added to it, (b) Singularity spectrum produced for the signal in (a)

From previous tests, we know that the sine wave produces only a dot on the singularity spectrum. However from the results above, it is clearly seen that once a certain type of noise - which in this case is the triangular pulse - is added to the signal the singularity spectrum changes. Convolution of the sine waves to these triangular pulses causes a spectrum of points to be generated rather than one point. The hypothesis that the study tests is that if the frequency of occurrence of the noise is higher the resulting signal will be more irregular.

When noise in the form of triangular pulses that repeat every 0.002 seconds are added to the signal, the singularity spectrum produces the lowest Holder exponent value ( $\alpha = - 2.939$ ) when compared to the other signals. This means that it is the most irregular signal in this group. This agrees with the hypothesis as this signal has the highest number of triangular pulse noise added to it. However, this trend does not follow through when the repetition of the triangular pulse is reduced; the level of irregularity of the signal does not decrease in the same order.

As it turns out, the triangular pulse repeated every 0.003 seconds produced a singularity spectrum with the highest set of Holder exponent values rather than the one with the noise repeated every 0.004 seconds. Therefore, the results show that this signal is the least irregular signal in this group of signals that were tested. These results indicate that it is in fact the positions at which the triangular pulse convolves with the sine wave that affects the singularity spectrum more than the number of times the triangular pulse convolves with the signal. This is because the singularities seen in Figure 25 can be observed to exhibit a much less rapid change in frequency as compared to the singularities produced in Figure 24 and Figure 26.

#### 4.1.4 Concatenate two sine signals of different frequencies

1) Freq of Sine wave1 = 100Hz. Freq of Sine wave2 = 10Hz

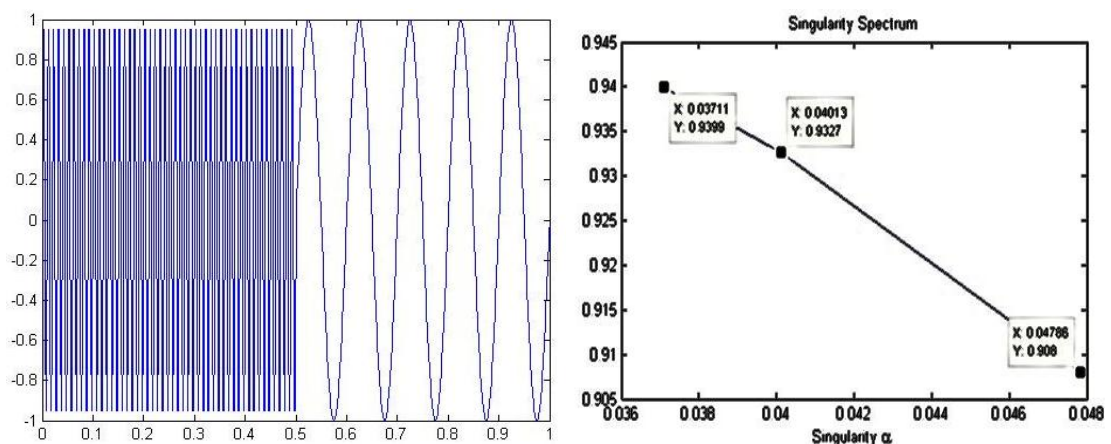


Figure 33: (a) 100Hz sine wave concatenated with a 10Hz signal, (b) Singularity spectrum produced

2) Freq of Sine wave1 = 100Hz Freq of Sine wave2 = 40Hz

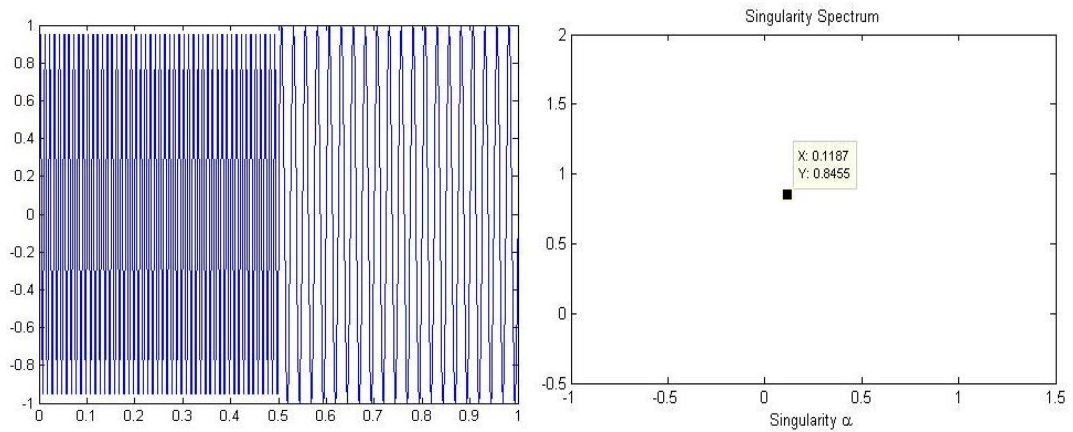


Figure 34: (a) 100Hz sine wave concatenated with a 40Hz signal, (b) Singularity spectrum produced

3) Freq of Sine wave1 = 100Hz Freq of Sine wave2 = 50Hz

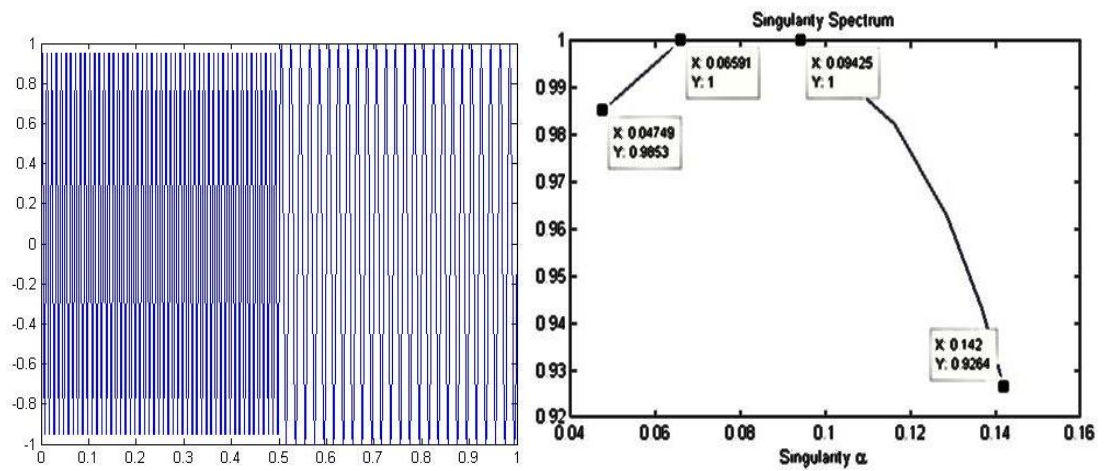


Figure 35: (a) 100Hz sine wave concatenated with a 50Hz signal, (b) Singularity spectrum produced

4) Freq of Sine wave1 = 100Hz Freq of Sine wave2 = 60Hz

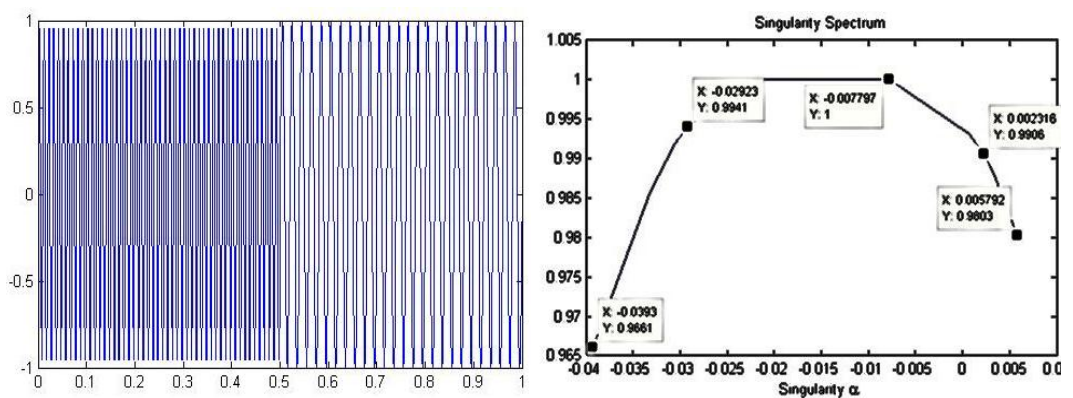


Figure 36: (a) 100Hz sine wave concatenated with a 60Hz signal, (b) Singularity spectrum produced

In all the tests that were done in this category, the signals were concatenated at 0.5s. The first signal in all cases was a 100Hz sine wave and it was concatenated with sine waves of frequencies 10Hz, 40Hz, 50Hz and 60Hz. From the study's understanding, the singularity spectrum should at least produce two points since two different signals are merged. However, taking the results of the concatenation of the 100Hz signal to the 10Hz signal, three singularities exist. This is due to the existence of signals with two different frequencies plus the point where the signals concatenate ( $t=0.5s$ ) which causes the other singularity. The concatenation of the 100Hz to the 50Hz and 60Hz signals produces a singularity spectrum with more than three points. This highlights that at  $t=0.5s$  more than one singularity exists compared to when the 100Hz signal was concatenated to a sine wave with a relatively smaller frequency of 10Hz.

However, the concatenation of the 40Hz signal to the 100Hz signals generates a singularity spectrum with only one point. This could be due to a perfect transition between the signals at  $t=0.5s$ .

#### 4.1.5 Addition of two sine waves in the same time period

In this test, a 100Hz sine wave which was sampled at 10 times its frequency for a time period of 0.5 seconds was added with other sine waves with frequencies of 10Hz, 20Hz, 30Hz and 40Hz. First the singularity spectrum of just the 100Hz sine wave is shown below.

##### 1. 100Hz signal

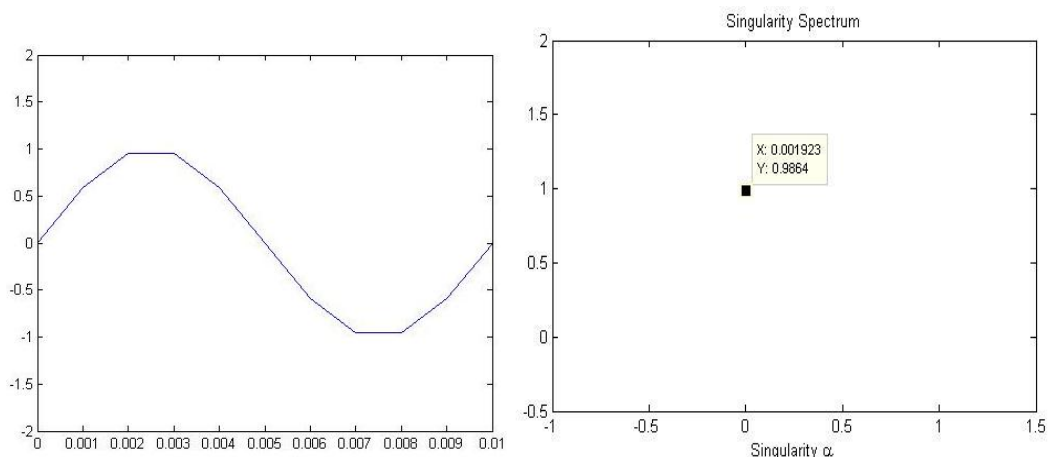


Figure 37: (a) A part of the 0.5 seconds long 100Hz sine wave (b) Singularity spectrum produced for the sine wave in (a)

2. Addition of 100Hz sine wave to 10Hz sine wave

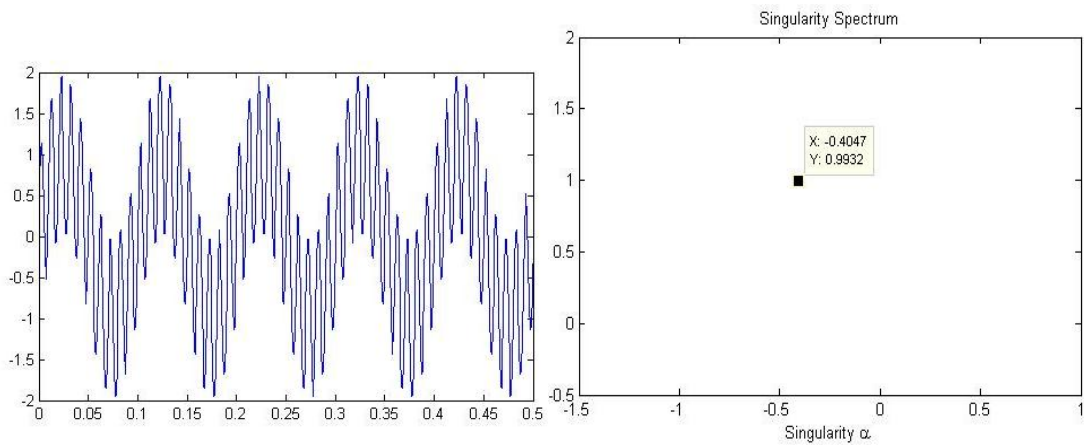


Figure 38: (a) 100Hz signal added to a 10Hz signal (b) Singularity spectrum produced for the sine wave in (a)

3. Addition of 100Hz sine wave to 20Hz sine wave

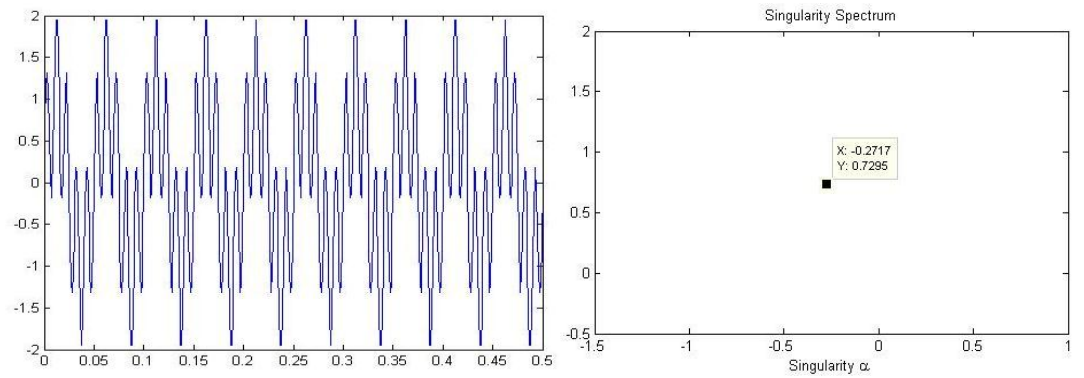


Figure 39: (a) 100Hz signal added to a 20Hz signal (b) Singularity spectrum produced for the sine wave in (a)

4. Addition of 100Hz sine wave to 20Hz sine wave

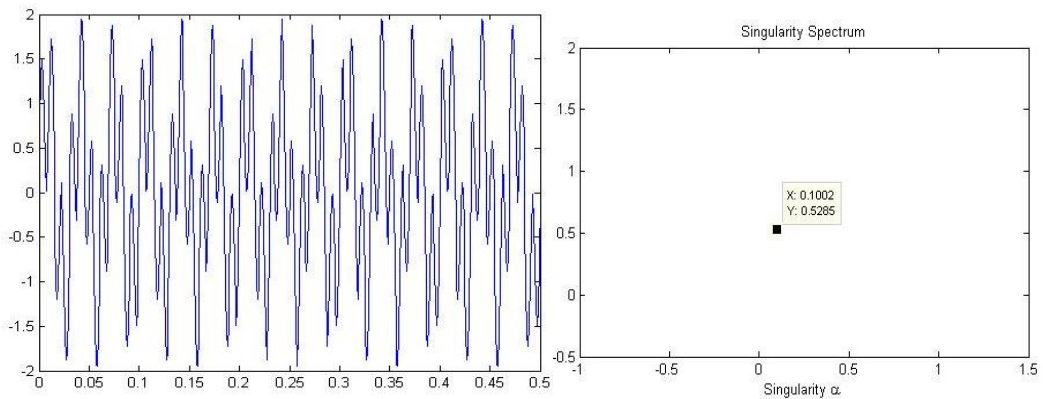


Figure 40: (a) 100Hz signal added to a 30Hz signal (b) Singularity spectrum produced for the sine wave in (a)

## 5. Addition of 100Hz sine wave to 40Hz sine wave

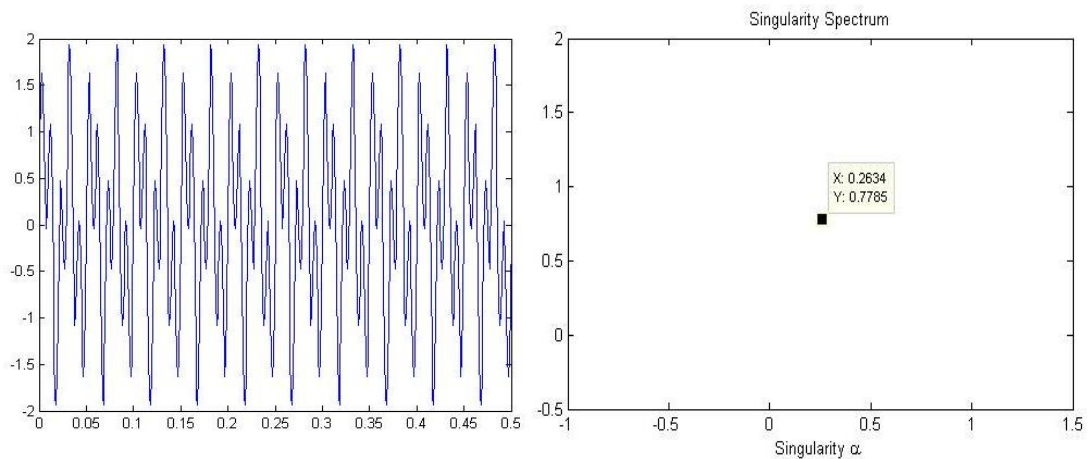


Figure 41: (a) 100Hz signal added to a 40Hz signal (b) Singularity spectrum produced for the sine wave in (a)

The first signal, the 100Hz sine wave signal produces a dot on the singularity spectrum as expected. From this test, the study intended to find out what the results will be if this signal was added to another sine wave of a different frequency. The study expected two points on any singularity spectrum produced due to the existence of signals with two different frequencies. However the results above show that the addition of two sine waves results in only a dot on the singularity spectrum. A pattern on the Holder exponents can also be observed as the dot moves from the most singular point for the addition of 100Hz sine wave to the 10Hz sine wave ( $\alpha = -0.4047$ ) to the least singular point for the addition of 100Hz sine wave to the 40Hz sine wave ( $\alpha = 0.2634$ ). One look at any of signals tested above gives the impression that there will be more than one holder exponent as they exhibit a lot of transients. However, this test proves that the addition of two smooth signals result in a signal with one singularity.

## 4.2 Results and analysis from seismic modelling

The seismic models that were created were made in such a way to test how the singularity spectrum changes when the following three factors were changed:

1. Reservoir Fluid
2. Thickness of the layers
3. Stratigraphy

#### 4.2.1 Response of singularity spectrum towards change in Reservoir Fluid

Since the main aim of seismic exploration activities is to aid with the detection of hydrocarbons, it is important to see how the singularity spectrum is affected with changes to the reservoir fluids. The three reservoir fluids that were modelled were oil, gas and water. The singularity spectrum that was generated from the fractal analysis was for a frequency range of 20 – 200 Hz using the ‘Morlet – analytic’ wavelet. In order to capture a wide range of weak and strong transients, the moment order,  $q$ , was selected for a range of +6 to -6 with 20 different ‘ $q$ ’ values in between them.

The Ricker wavelet which was used had a centre frequency of 60Hz and the reflectivity series was sampled at 0.002 seconds for every reservoir fluid. Since the current model is being tested only for reservoir fluids, the rest of the two parameters i.e. thickness of each layer and number of layers were kept constant. In this case, the thickness of the layers was kept at 30m each in a 4 layer seismic model.

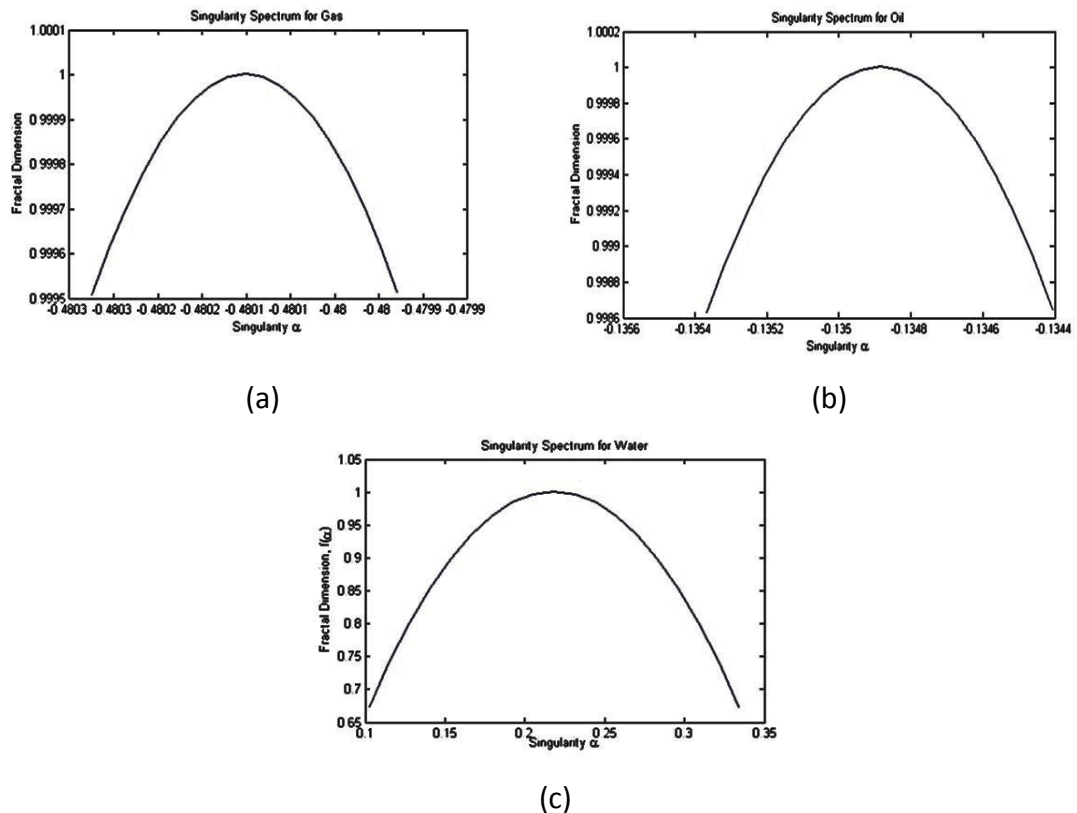


Figure 42: (a) Singularity Spectrum for Gas (b) Singularity Spectrum for Oil (c) Singularity spectrum for Water

Table 2: Singularity spectrum attributes for different reservoir fluids

<b>Reservoir Fluid</b>	<b><math>\alpha_{\text{peak}}</math></b>	<b>Asymmetry</b>	<b>Width</b>
<b>Oil</b>	<b>-0.13488</b>	<b>1.04255</b>	<b>9.6*10<sup>-4</sup></b>
<b>Gas</b>	<b>-0.48015</b>	<b>1</b>	<b>3.4*10<sup>-4</sup></b>
<b>Water</b>	<b>0.21826</b>	<b>0.9985</b>	<b>0.23157</b>

#### 4.2.2 Response of singularity spectrum towards change in Reservoir Fluid

To test the reliability of using the singularity spectrum for the detection of hydrocarbons, for each of the reservoir fluid, the thickness of the layers were changed. The thicknesses of the layers were kept at 30m, 40m and 50m. Just as the previous test, the wavelet that was used for the fractal analysis was the ‘Morlet – analytic’ wavelet. The range of frequency covered by the test was from 20 – 200 Hz. In order to capture a wide range of weak and strong transients, the moment order, q, was selected for a range of +6 to -6 with 20 different ‘q’ values in between them. The Ricker wavelet used as the source wavelet again had a centre frequency of 60Hz and the reflectivity series was sampled at 0.002 seconds for every reservoir fluid. The results obtained are tabulated below.

Table 3: Singularity spectrum attributes for each reservoir fluid at different thicknesses

<b>Reservoir Fluid</b>	<b>Thickness of layer(m)</b>	<b><math>\alpha_{\text{peak}}</math></b>	<b>Asymmetry</b>	<b>Width</b>
<b>Oil</b>	<b>30</b>	<b>-0.13488</b>	<b>1.04255</b>	<b>9.6*10<sup>-4</sup></b>
<b>Oil</b>	<b>40</b>	<b>-0.13488</b>	<b>1.04255</b>	<b>9.6*10<sup>-4</sup></b>
<b>Oil</b>	<b>50</b>	<b>-0.13488</b>	<b>1.04255</b>	<b>9.6*10<sup>-4</sup></b>
<b>Gas</b>	<b>30</b>	<b>-0.48015</b>	<b>1</b>	<b>3.4*10<sup>-4</sup></b>
<b>Gas</b>	<b>40</b>	<b>-0.48015</b>	<b>1</b>	<b>3.4*10<sup>-4</sup></b>
<b>Gas</b>	<b>50</b>	<b>-0.48015</b>	<b>1</b>	<b>3.4*10<sup>-4</sup></b>
<b>Water</b>	<b>30</b>	<b>0.21826</b>	<b>0.9985</b>	<b>0.23157</b>
<b>Water</b>	<b>40</b>	<b>0.21826</b>	<b>0.9985</b>	<b>0.23157</b>
<b>Water</b>	<b>50</b>	<b>0.21826</b>	<b>0.9985</b>	<b>0.23157</b>

### 4.2.3 Response of singularity spectrum towards change in stratigraphy

This study also looks at the effects a change in stratigraphy would have on the singularity spectrum produced by the reservoir fluids. The number of layers of the reservoir fluids in each model was varied between 4, 6 and 8 layers. The ‘Morlet – analytic’ wavelet was used for the fractal analysis and the frequency of analysis was from 20 – 200Hz. The range of moment order,  $q$ , was set from +6 to -6. In between those two values, data for 20 different ‘ $q$ ’ values were produced to capture a wide range of transients accurately. The source wavelet for the reflectivity series was a Ricker wavelet with a centre frequency of 60Hz. The reflectivity series for each reservoir model was sampled at 0.002 seconds.

Table 4: Singularity spectrum attributes for different number of layers of gas

<b>Reservoir Fluid</b>	<b>No. of Layers</b>	<b><math>\alpha_{\text{peak}}</math></b>	<b>Asymmetry</b>	<b>Width</b>
<b>Oil</b>	<b>4</b>	<b>-0.13488</b>	<b>1.04255</b>	<b><math>9.6 \times 10^{-4}</math></b>
<b>Oil</b>	<b>6</b>	<b>-0.13488</b>	<b>1.04255</b>	<b><math>9.6 \times 10^{-4}</math></b>
<b>Oil</b>	<b>8</b>	<b>-0.13488</b>	<b>1.04255</b>	<b><math>9.6 \times 10^{-4}</math></b>
<b>Gas</b>	<b>4</b>	<b>-0.48015</b>	<b>1</b>	<b><math>3.4 \times 10^{-4}</math></b>
<b>Gas</b>	<b>6</b>	<b>-0.48015</b>	<b>1</b>	<b><math>3.4 \times 10^{-4}</math></b>
<b>Gas</b>	<b>8</b>	<b>-0.48015</b>	<b>1</b>	<b><math>3.4 \times 10^{-4}</math></b>
<b>Water</b>	<b>4</b>	<b>0.21826</b>	<b>0.9985</b>	<b>0.23157</b>
<b>Water</b>	<b>6</b>	<b>0.21826</b>	<b>0.9985</b>	<b>0.23157</b>
<b>Water</b>	<b>8</b>	<b>0.21826</b>	<b>0.9985</b>	<b>0.23157</b>

### 4.2.4 Analysis of results from seismic modelling

The seismic modelling is done to identify if there is a possibility of using fractal analysis and singularity spectrum to characterize each reservoir fluid. From our understanding, gas is the most irregular of the three as its atoms are constantly moving and colliding with each other. Therefore, gas should have the lowest  $\alpha$  values signalling the highest irregularity.

Meanwhile, the study also hypothesised before the modelling that oil and gas should have  $\alpha$  values that are close to each other as they are both in the liquid form. Also, in comparison to gas, it is expected that the  $\alpha$  values of both liquids should be higher signalling that it is more regular in comparison to gas. This is because we know atoms

in the liquids do not contain as much energy as gases and much less collision occurs between the atoms.

From the plots above, we have three different criteria i.e.  $\alpha_{\text{peak}}$ , width and asymmetry from which the spectra can be analysed. Before dealing with those three criteria, just taking a look at the three spectra reveals that gas contains the strongest singularities. This is because its spectrum contains the smallest  $\alpha$  values in the region of -0.48 compared to water and gas. In the same light, water contains the weakest singularities of the three having the highest  $\alpha$  values in the region of 0.1 to 0.35.

Now, looking just at  $\alpha_{\text{peak}}$  value, gas has that particular singularity  $\alpha_{\text{peak}} = -0.48015$  occurring the most in this model. In other words, a stronger singularity - with regards to the other two fluids – makes up most of the seismic model of gas. Meanwhile water has the highest  $\alpha_{\text{peak}}$  value of 0.21826 among the three meaning a weaker singularity describes this reservoir fluid. This agrees with the initial assumption made by the study that gas will have the highest energy content which will be displayed by having the smallest  $\alpha$  value of the three reservoir fluids.

Moving on to the next characteristic, asymmetry, gas has an asymmetry value of 1. This in other words means that the spectrum is symmetrical. What this means in terms of singularities present in the gas model is that the weaker and stronger singularities are evenly distributed on both sides of  $\alpha_{\text{peak}}$ . For oil on the other hand, its asymmetry is 1.04255. This means that there are more singularities to the left of  $\alpha_{\text{peak}}$ . Oil in this model therefore contains more singularities that are stronger than  $\alpha_{\text{peak}}$ . The opposite takes place with water in this seismic model. Since it has an asymmetry value of 0.9985 which is smaller than one, more singularities are found to the right of the  $\alpha_{\text{peak}}$  value.

Width is the final characteristic that is investigated from the singularity spectra. Water generates the spectrum that is widest meaning its singularities are more spread out. This means that there are a lot of different singularities in the seismic model for water. Gas on the other hand has the smallest width meaning that it has fewer singularities as a whole to describe it. This could be down to the fact that most of the gas particles are at a high energy level described by  $\alpha_{\text{peak}}$  and only a small amount of particles either exceed or is below this singularity level.

The interesting thing noted from the three different factors that were tested i.e. reservoir fluid type, thickness of layer and stratigraphy, even with the change in these

factors each reservoir fluid produced the same singularity spectrum for their respective models. This shows that the different reservoir fluids can definitely be differentiated from the seismic models alone. These are some promising results and shows that there is potential in detecting and delineating a reservoir fluid from seismic data.

### **4.3 Results and analysis from the testing of the direct detection and delineation method on actual seismic data**

Since the seismic modelling provided some positive results by proving that reservoir fluids can be characterised by its own specific singularity spectrum, the study proceeded to test the direct detection and delineation method with the seismic data obtained from a real wild cat well. Due to the confidential nature of these wells and its reports, this well will be called Well X or WX for short. From the well summary, geologists have confirmed the presence of gas in five reservoirs and also one reservoir with oil. These reservoirs are listed out below:

Table 5: List of reservoirs and reservoir fluid

Reservoir Name	Reservoir Fluid
WX-1	Gas
WX-2	Gas
WX-3	Gas
WX-4	Gas
WX-5	Gas
WX-6	Oil

With this data, the study sets out to test and prove the direct detection and delineation method. From the seismogram that was generated using Petrel, the reflection coefficients were extracted and convolved with a 60Hz Ricker wavelet to produce the seismic trace on MATLAB. The next step is to upsample the seismic trace. The original data was sampled at 4ms and the space between each sample was approximately 1.5 - meters. The data was upsampled by a factor of 20 and each window contains two original samples or in other words 40 samples after the upsampling. Therefore, the depth of analysis of each window is approximately 3 meters.

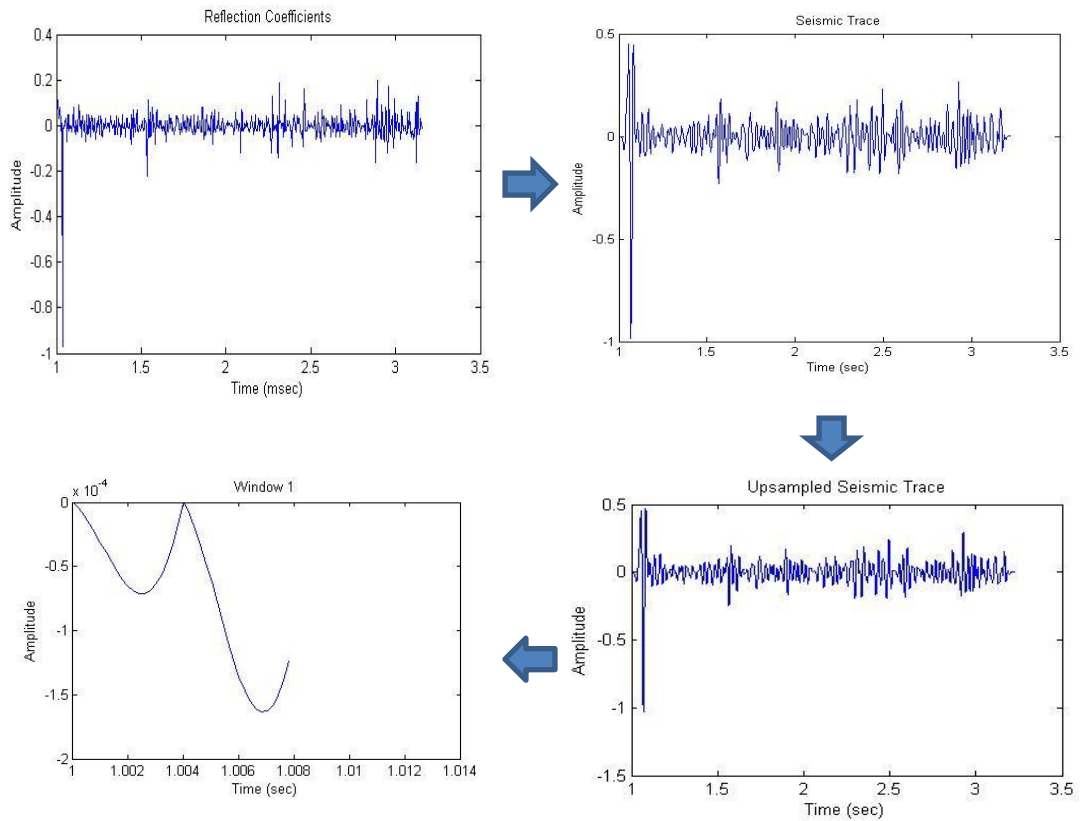


Figure 43: A graphical illustration of the steps to obtain windows

Once all the windows have been obtained, fractal analysis is performed on these windows and the  $\alpha_{\text{peak}}$  values are extracted and plotted.

#### 4.3.1 Detection of the reservoirs

Continuous wavelet transform is then done on this plot. The plot should indicate larger coefficient values at the windows where the reservoirs are located. The wavelet used for the continuous wavelet transform is ‘Morlet – analytic’ wavelet in order to be consistent with the wavelet that was used as the basis to obtain the singularity spectrum of each window.

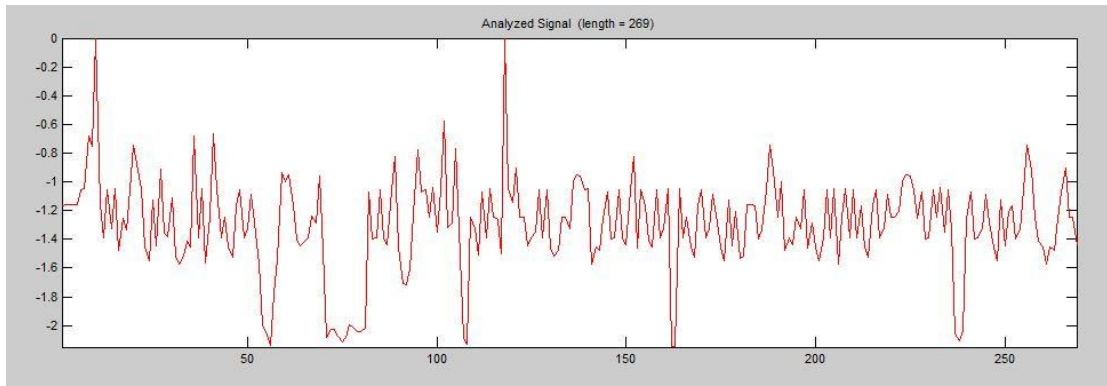


Figure 44:  $\alpha_{\text{peak}}$  plot of all the windows

The continuous wavelet of the  $\alpha_{\text{peak}}$  proved to contain high energy at the areas where gas and oil were present.

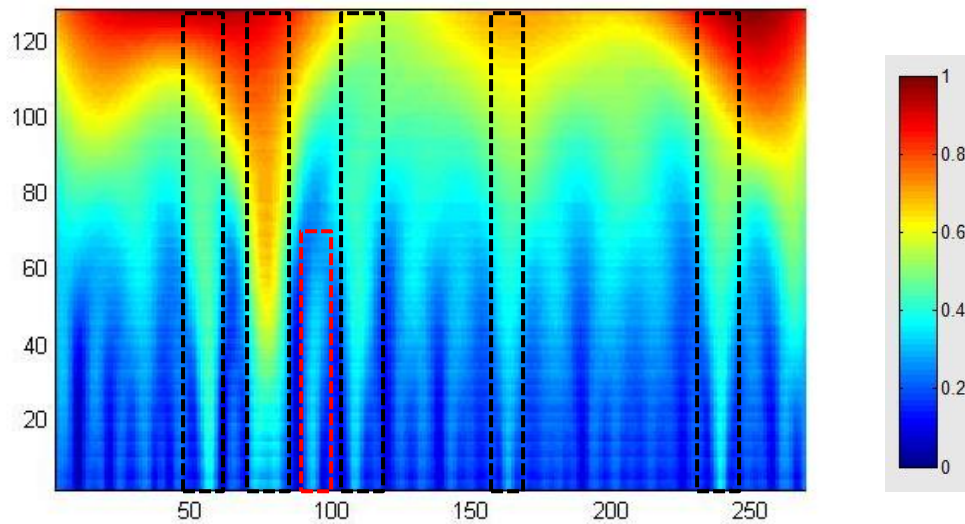


Figure 45: Continuous wavelet transform with the regions where gas and oil are present. Gas reservoirs are highlighted by the black boxes while oil reservoir is highlighted by the red box

The results obtained from the continuous wavelet transform were positive. As was expected, the reservoirs where gases were present are highlighted as singularities. This is due to the high energy content of gas particles. The gas reservoirs have been marked with black dotted boxes in the figure above. While other regions of the transform do have maxima points at the lower scales, from our study, we know that for a singularity to exist at a certain time,  $t_0$  we must be able to construct a modulus maxima line. For this to happen, maxima points must exist from higher scales right

down to the finer scales as mentioned in section 2.4.1.2 of this study. It is clear that the reservoirs containing gas fit these criteria.

The dotted red box in figure 39 meanwhile points to the oil reservoir of this well. Although in this section a maxima line cannot be plotted, when compared to other regions of the continuous wavelet transform, this region is clearly brighter indicating the presence of a hydrocarbon and in this case, oil. We know that the energy content of oil is generally lower than gas; however from the reports we learn that in the WX-6 reservoir, the oil content is really low. The volume of oil found is not economically viable to be recovered from the reservoir. The volume of oil in the reservoir could also have had an effect on the results.

### 4.3.2 Delineation of Reservoirs

With the detection of the reservoirs completed. The study moved to the delineation phase. As mentioned in the methodology section, for delineation other spectral attributes namely asymmetry and width will be included together with  $\alpha_{\text{peak}}$  values. The study will list out the singularity spectrum generated at each reservoir followed by an analysis.

#### 4.3.2.1 Delineation of reservoir WX-1

In the first reservoir, the gas is found primarily in window 55 but windows 54 and 56 have been included as some interesting features are discovered for analysis.

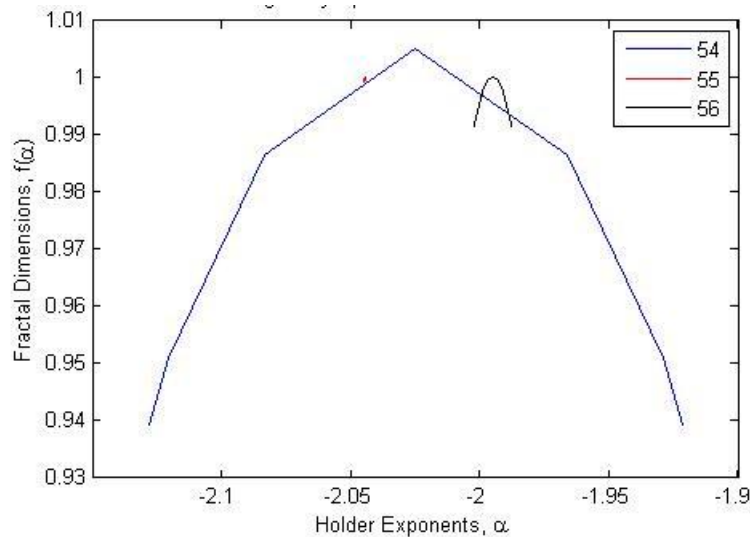


Figure 46: Singularity spectrum of windows 54, 55 and 56

Figure 41 below is just an enlarged version of the singularity spectrum of window 55 from figure 40.

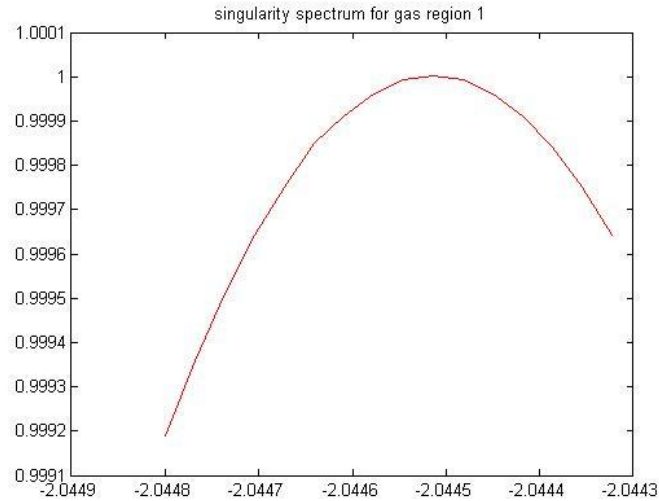


Figure 47: Window 55 or WX-1

We have managed to prove that the regions where reservoirs are found, the energy content is high and this is reflected by a smaller  $\alpha_{\text{peak}}$  value. Now fractal analysis was done on these regions and the singularity spectrum attributes for these regions are studied. The study expects the singularity spectrum of the window where the reservoir is located should also have a low  $\alpha_{\text{peak}}$  value. The study also aims to study how the values of width and asymmetry of the singularity spectrum changes.

Table 6: Spectral attributes of related windows

Window No.	$\alpha_{\text{peak}}$	Width	Asymmetry
<b>54</b>	-2.02472	0.206592	0.999903
<b>55</b>	-2.04451	0.000477	1
<b>56</b>	-1.99495	0.014204	1

From the results obtained, we do observe that window 55 has the smallest  $\alpha_{\text{peak}}$  value ( $\alpha_{\text{peak}} = -2.04451$ ) of the windows surrounding it. This agrees with what the study's hypothesis since this is the region with the highest gas content compared to the surrounding windows. Meanwhile, window 54 is the start of the reservoir and we see that the energy of this window is increasing. In other words, the  $\alpha_{\text{peak}}$  of window 54 ( $\alpha_{\text{peak}} = -2.02472$ ) is low and is close to the value of that seen in window 55. Also, window 56 being the end of reservoir WX-1 produces a singularity spectrum that

moves to the right of window 55 with ( $\alpha_{\text{peak}} = -1.99495$ ). This indicates with the reduction of gas in the window, the energy content within it also decreases. This is an interesting pattern that was identified from the results.

The value of width of each singularity spectrum also indicates an interesting pattern. The singularity spectrum of window 55 has a significantly smaller width of 0.000477 as compared to window 54 (0.206592) and window 56 (0.014204). This could prove to be a very valuable singularity spectrum attribute for delineation. The reduction in the width of window 55 could serve as an indication that there is only one type of material in this region and in our case, gas. Singularity spectra of windows 54 and 56 have much larger widths in comparison since these windows are both the start and the end of the reservoir respectively and thus only part of the windows are made up of gas while the other could be any other subsurface rock or material.

From the seismic modelling in the previous section, we found that the asymmetry of gas was 1. The results from windows 54 to 56 also have asymmetry values close to 1. This could also serve as an indication for the presence of gas. Results from other reservoirs should indicate if indeed asymmetry could also be used as a tool for delineation.

#### 4.3.2.2 Delineation of reservoir WX-2

WX-2 is a thicker reservoir of gas compared to WX-1. The singularity spectrum of the first few windows and the last few windows of reservoir WX-2 are shown below and analysed accordingly.

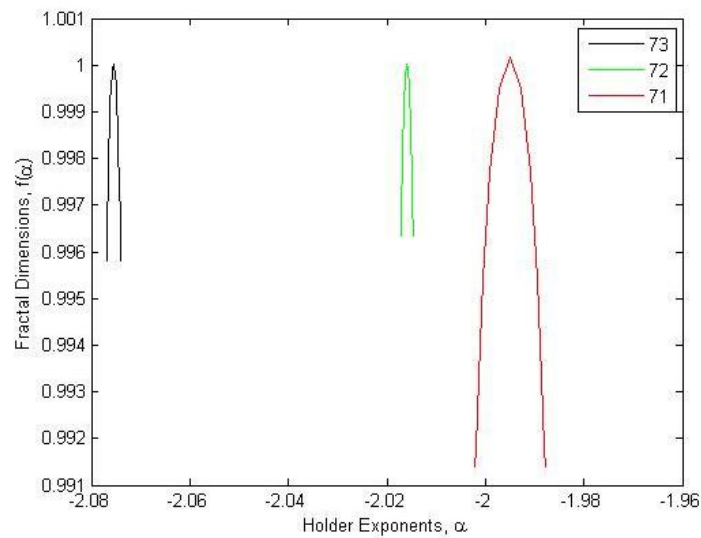


Figure 48: Singularity spectrum of windows 73, 72 and 71

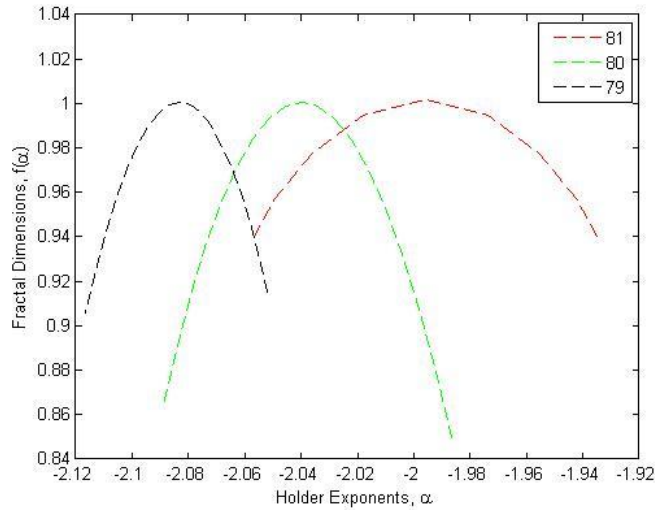


Figure 49: Singularity spectrum of windows 81, 80 and 79

Figure 42 above is the windows that depict the start of reservoir WX-2 as well as the progression into the reservoir. Meanwhile figure 43 shows the singularity spectra of windows from within the reservoir towards the end of the reservoir WX-2.

Table 7: Spectral attributes related to windows at the start of WX-2

Window No.	$\alpha_{\text{peak}}$	Width	Asymmetry
<b>71</b>	-1.99495	0.014204	1
<b>72</b>	-2.01591	0.002587	1
<b>73</b>	-2.07547	0.002954	1

The table above summarizes the singularity spectral attributes of the spectra from figure 42. Window 71 being the starting point of the reservoir shows has a  $\alpha_{\text{peak}}$  value of -1.99495 and we observe that the following window moves to the left indicating an increase in energy as it goes into the gas reservoir producing a  $\alpha_{\text{peak}}$  of -2.01591. Here we also observe that from window 71 to 72 there is a drop in the width of the spectra from 0.014204 to 0.002587. These results show a similar trend as we had observed from WX-1. While the  $\alpha_{\text{peak}}$  values have demonstrated an increase in irregularity or energy from the start of the reservoir as we move into the reservoir, it has also shown that the width decreases when the window moves from the start of the reservoir into the reservoir. This shows the window is moving from a region with a mixture of gas and other subsurface material to a purely gas containing reservoir.

The pattern also follows through as we move deeper into the reservoir, shown by window 73. It has the lowest  $\alpha_{\text{peak}}$  value of the three windows showing the highest irregularity of the three. The value of width which is 0.002954 stays close to the value observed in from window 72 indicating we are still in the gas reservoir. To sum up the results, we see that the asymmetry of all three windows are 1, a pattern that is believed to be another indicator of presence of gas when used together with both  $\alpha_{\text{peak}}$  and width values. So far, both WX-1 and WX-2 have indicated similar patterns and have shown  $\alpha_{\text{peak}}$  values in the region of -2. These are positive results that show that delineation is possible with our method.

Table 8: Spectral attributes towards the end of reservoir WX-2

Window No.	$\alpha_{\text{peak}}$	Width	Asymmetry
<b>79</b>	-2.08312	0.065067	1.059427
<b>80</b>	-2.03981	0.102954	1.004200
<b>81</b>	-1.99582	0.12348	1

As mentioned previously, WX-2 is a thicker compared to WX-1, thus it is covered by more windows. Window 79 to 81 is a progression from within the reservoir towards the end of the reservoir. Again, results obtained are as expected. Seeing that window 79 is still very much in the reservoir, it has the lowest  $\alpha_{\text{peak}}$  of the three at -2.08312. Its width is also much smaller than the widths of the following two windows meaning that it is still in a region where it is made up of mainly one substance i.e. gas. Asymmetry values are also in the region of 1 which is – by looking at the results from WX-1 and in Table 7 from WX-2 – a possible indication towards existence of gas. Since there are three more gas reservoirs, whether these results can be used as a marker to pinpoint the existence of gas can be summarised at the end.

#### 4.3.2.3 Delineation of reservoir WX-3

WX-3 is described by three windows, windows 107 to 109. The spectra obtained in these windows are in the following figures.

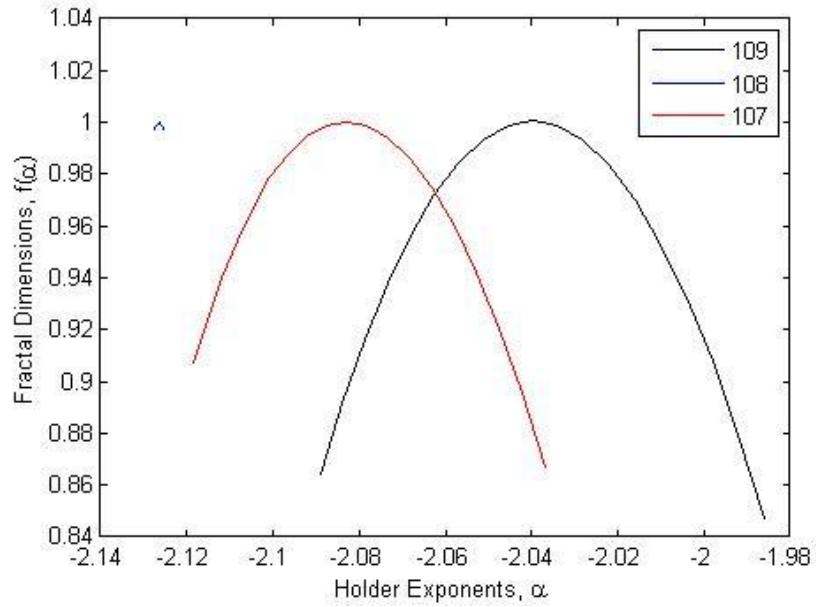


Figure 50: Singularity spectrum of windows 107, 108 and 109

An enlarged view of window 108 can be seen in figure 45 below.

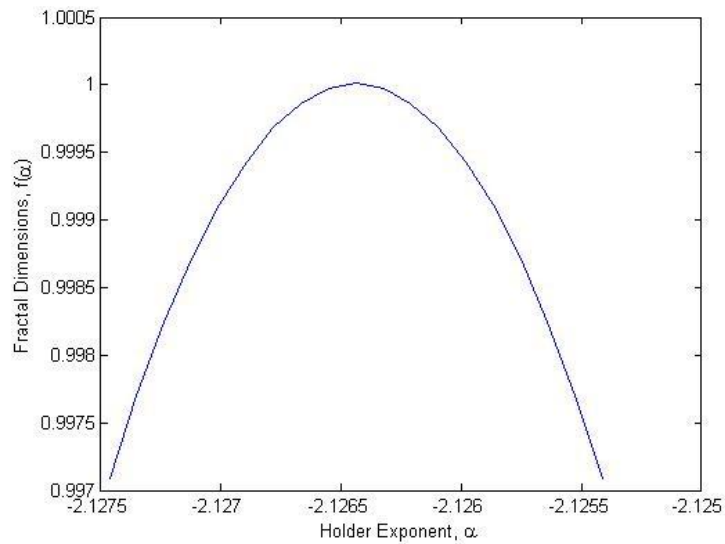


Figure 51: Singularity spectrum of window 108

From the analysis of WX-1 and WX-2, looking at figure 44, we see a similar trend. These results look increasingly positive in proving that the delineation method can be used to delineate gas from the seismic data.

Table 9: spectral attributes of windows related to WX-3

Window No.	$\alpha_{\text{peak}}$	Width	Asymmetry
<b>107</b>	-2.08305	0.081493	1.020400
<b>108</b>	-2.12644	0.002053	1
<b>109</b>	-2.03981	0.102954	0.916025

The results of WX-3 indicate what we have seen from WX-1 and WX-2. As we move from the start of the reservoir at window 107, the  $\alpha_{\text{peak}}$  value decreases from -2.08305 to -2.12644 as it moves into the reservoir at window 108. An increase in irregularity is what these results indicate and this is exactly what was expected since we are moving into the gas-filled region. Window 109 then has its  $\alpha_{\text{peak}}$  moving back to the right showing that it's coming to the end of the reservoir WX-3.

Looking at the values obtained for width, as we move into the reservoir at window 108, the width drops from 0.081493 at window 107 to 0.002053. This significant drop has been observed in all of the reservoirs before and is proving to be a useful delineation tool. It shows that as we move into the region of mainly gas, the width decreases while when the region is a mixture of gas and other subsurface material, the width increases. Finally, the asymmetry value just as from reservoirs WX-1 and WX-2 has remained in the region of 1. Asymmetry is a spectral attribute that has proven that it can be used as a delineation tool when used together with  $\alpha_{\text{peak}}$  and width values.

#### 4.3.2.4 Delineation of reservoir WX-4

Reservoir WX-4 is made up of gas as well. It is described by the windows 162, 163 and 164. The singularity spectra of the windows again move to the left from the start of the reservoir to the middle of the reservoir. The singularity spectrum of the final window, then moves back to the right signalling that it is leaving the gas reservoir. It can be observed in the following figure.

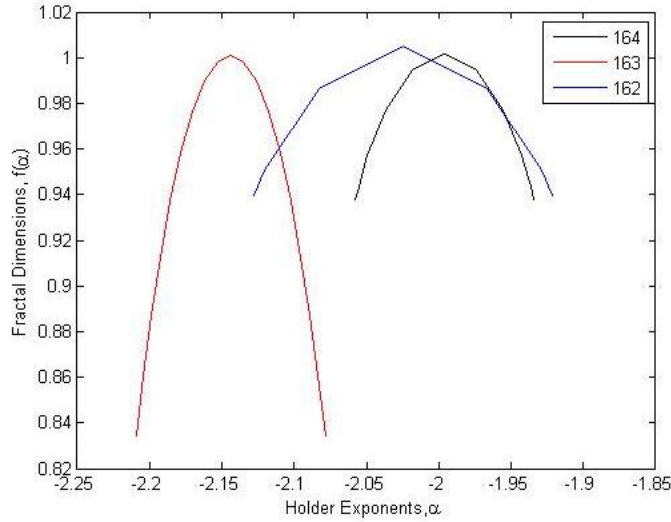


Figure 52: Singularity spectra of windows 162-164

Table 10: Spectral attributes of windows in reservoir WX-4

Window No.	$\alpha_{\text{peak}}$	Width	Asymmetry
<b>162</b>	-2.02472	0.206582	1
<b>163</b>	-2.14393	0.130817	1
<b>164</b>	-1.99582	0.12348	1

The  $\alpha_{\text{peak}}$  value decreases from window 162 to window 163. This is expected since we move from the start of the gas region into the actual gas region. It is interesting to note that the value for  $\alpha_{\text{peak}}$  remained within the region of -2.0 to -1.9 in all the previous reservoirs as well as in reservoir WX-4. This together with the pattern demonstrated by width, whereby the width of the singularity spectrum decreases significantly from the start of the reservoir to the middle of the reservoir are two strong points that can be used for the delineation of gas.

These two attributes merged with the final attribute, asymmetry is three characteristics of the singularity spectrum that can help with the identification of gas. Asymmetry has remained at the value of 1 or close to 1 for all previous reservoirs as well as in reservoir WX-4. This indicates that gas produces a symmetrical spectrum meaning that its singularities are spread out evenly between the left and right side of  $\alpha_{\text{peak}}$ . This if we recall from section 4.2 of this study is what was observed from the seismic modelling results as well.

#### 4.3.2.5 Delineation of reservoir WX-5

WX-5 is the final reservoir in the WX well where gas is present. It is again clear that when we move into the gas reservoir (window 238 in this case) the width and the  $\alpha_{\text{peak}}$  decreases. An analysis of this reservoir can be seen after the following figure.

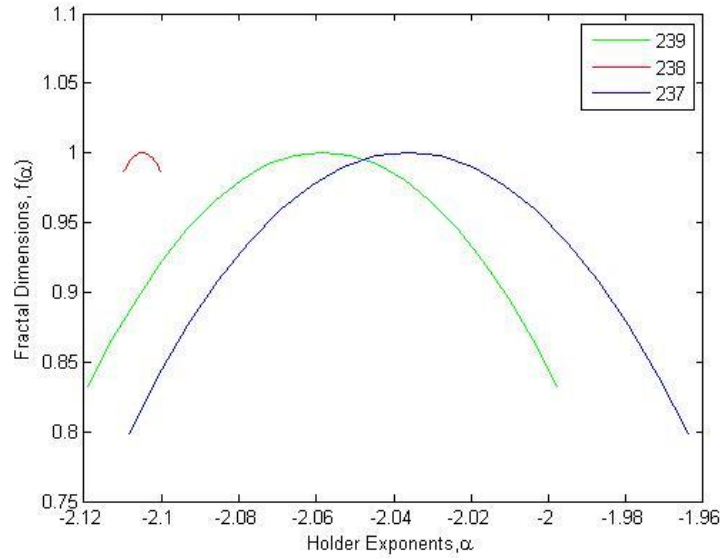


Figure 53: Singularity spectra of windows 237, 238 and 239

Table 11: Spectral attributes of the spectrums for reservoir WX-5

Window No.	$\alpha_{\text{peak}}$	Width	Asymmetry
<b>237</b>	-2.03628	0.144576	1
<b>238</b>	-2.10497	0.009616	1
<b>239</b>	-2.05840	0.121146	1

Coming to the final gas reservoir in well WX-5, we have now five sets of data that have produced extremely positive results to prove that delineation is possible. In this region, we once again see that from the start of the reservoir at window 237 to the middle of the reservoir at window 238,  $\alpha_{\text{peak}}$  reduces from -2.03628 to -2.10497. This not only shows that the decrease in value, but the fact that the  $\alpha_{\text{peak}}$  itself is within the range of -2 is an interesting point to note as well. Then, at the end of the reservoir the  $\alpha_{\text{peak}}$  value increases again to -.205840 showing that it has departed from a region of high irregularity.

The width of the singularity spectrum of window 238 which is 0.009616 is much smaller than the windows surrounding it. Much like what has been observed from reservoirs WX-1 to WX-4, the width is much smaller at the region where the gas is most prominent. Finally, asymmetry value has consistently stayed at 1 or a small deviation from 1 showing that gas produces a spectrum that has evenly distributed singularities.

In the conclusion of this section, the study will put together all the attributes from wells WX-1 to WX-4 together to summarise the delineation of gas.

#### 4.3.2.6 Delineation of reservoir WX-6

The WX well has one oil reservoir sitting within windows 91-93.

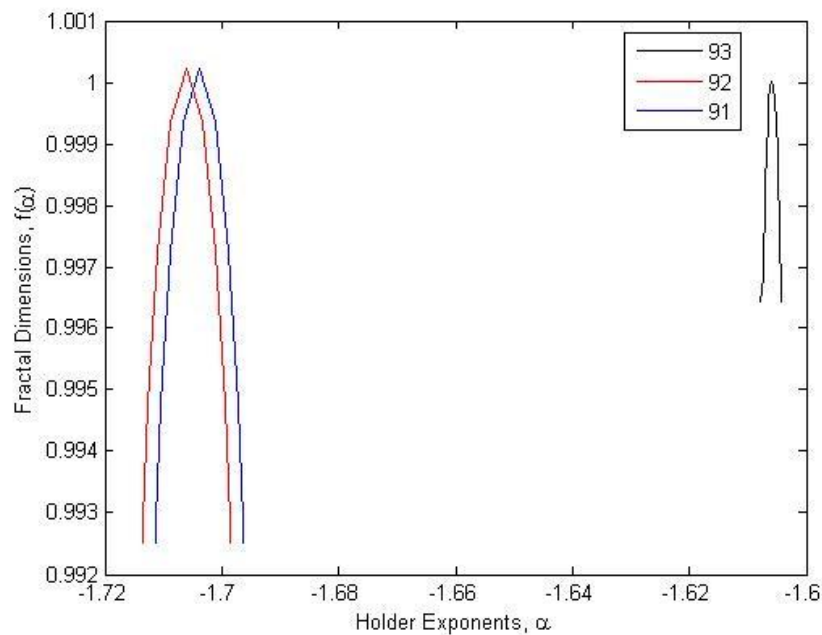


Figure 54: Singularity spectra of windows 91, 92 and 93

Although there is only one reservoir containing oil in this well, the study has still done an analysis based on the spectral attributes that are listed out in the table below.

Table 13: Spectral attributes of the spectra for reservoir WX-6

Window No.	$\alpha_{\text{peak}}$	Width	Asymmetry
<b>91</b>	-1.70383	0.017036	1.266029
<b>92</b>	-1.71331	0.017047	1.269845
<b>93</b>	-1.60587	0.003555	1.253554

The study expected a same pattern as observed in the gas regions whereby the energy increases from the start of the reservoir to the position where it moves into the reservoir. This is because from the detection part of the study, the continuous wavelet transform in 4.3.1 shows a slight elevation of energy in the region of reservoir WX-6. An increase in energy correlates to a decrease in  $\alpha_{\text{peak}}$  value. Looking at window 91 and 92, this pattern is observed as we see the value of  $\alpha_{\text{peak}}$  decreasing from -1.70383 to -1.71331.

Meanwhile, the asymmetry value has remained in the region of 1.25 to 1.26 in the reservoir WX-6. As we recall from the seismic modelling, oil does have an asymmetry of more than 1. It has again been shown here.

However, in terms of width, the window where the reservoir starts (window 91) and the window where we move deeper into the reservoir (window 92) actually show a bigger width compared to that of window 93. This could mean that the oil has a mixture of other materials as well. However this is not clearly stated in the well report, therefore only an assumption can be made at this point.

#### 4.3.2.7 *Summarising the results from delineation*

The delineation method has clearly been proven to work for all the gas reservoirs in this well.

For  $\alpha_{\text{peak}}$  and asymmetry, the range of values can be seen as follows:

$$-2.1381 \leq \alpha_{\text{peak}} \leq -1.9958$$

$$0.916025 \leq \text{asymmetry} \leq 1.069975$$

The values of  $\alpha_{\text{peak}}$  have consistently remained in this region for all the windows related to gas reservoirs. The range between the  $\alpha_{\text{peak}}$  values is 0.1422. Meanwhile asymmetry has remained close to 1 and its range of values is 0.15395. These ranges are the limiting values of  $\alpha_{\text{peak}}$  and asymmetry delineation.

In addition to that, the pattern observed with the width could serve as an additional indication on whether we are approaching a gas reservoir. This is because from the results, we have seen that the width of the singularity spectrum of the window decreases from the area where the reservoir starts and as we move into the reservoir.

For the oil reservoir, the presence of just one oil reservoir dents the proving process. However, with the data provided by the well, the following summary can be made regarding the values of  $\alpha_{\text{peak}}$  and asymmetry:

$$-1.71331 \leq \alpha_{\text{peak}} \leq -1.60587$$

$$1.253554 \leq \text{asymmetry} \leq 1.269845$$

The values of  $\alpha_{\text{peak}}$  have remained in a range of 0.10744 while the asymmetry has a range of 0.01629. The small range of values is a good indication for a possibility of the application of the delineation method. However, since there is only one oil reservoir in well WX, we would only be able to ascertain that the delineation method can work for oil with the study of other wells where oil is present.

A future study also needs to be done to see if the limiting values seen for gas can be used to delineate gases in a region with similar stratigraphy and different stratigraphy to strengthen the ability of this delineation method.

## CHAPTER 5

### CONCLUSION AND RECOMMENDATIONS

#### 5.1 Conclusion

This study as a whole was divided into two phases whereby the first phase involved understanding the mathematics of the fractal analysis method used, which is the Wavelet Transform Modulus Maxima (WTMM) method. Fractal analysis was carried on signals that were generated on MATLAB and the singularity spectra obtained were analysed. Meanwhile, the second phase aimed on the development of the hydrocarbon detection and delineation algorithm. This included studying the changes on the singularity spectra on seismic models and later testing out the developed direct detection and delineation method on real seismic data.

At the end of the first phase of this study, it was clear that when fractal analysis is performed on different signals, changes can be observed on the singularity spectrum that is generated. Square waves have proven to be the most irregular signal when compared with sine and sawtooth waves of similar frequencies. Adding on to that, it amplitude changes in a signal do not affect the outcome of the singularity spectrum, only frequency changes do. Also, when two signals are merged – in two possible ways, concatenation and addition – the singularity spectra also produce different results. Concatenation of signals results in more than one singularity due to the fact that there is at least one singularity at the point where the two signals ‘meet’. Meanwhile, when two sine waves were added to each other, only a dot is observed on the singularity spectrum indicating that it is a monofractal signal thus resulting in only one singularity.

In the second phase of the study, seismic models were developed and fractal analysis was performed on these models. It helped to set the foundation for the development of the direct detection and delineation algorithm as the singularity spectra produced for oil, water and gas were analysed. These models were tested with three variables,

type of reservoir fluid, thickness of layers and stratigraphy. The most interesting discovery from the results of modelling was that each reservoir fluid produced its own distinct singularity spectrum. Not only that, the singularity spectrum for the respective reservoir fluids remained the same although other factors under test like thickness of the layers and stratigraphy changed.

Next, the spectral attributes of interest from the singularity spectra, namely  $\alpha_{\text{peak}}$ , and asymmetry were analysed. It was proven that gas is the most irregular of the three fluids as it produced the lowest  $\alpha_{\text{peak}}$  value of -0.48015. This agrees with our understanding since gas has higher energy content due to its atoms that are constantly moving and colliding with each other. While oil had the second highest irregularity with the  $\alpha_{\text{peak}}$  value of -0.13488 and finally followed by water ( $\alpha_{\text{peak}} = 0.21826$ ). The next attribute was asymmetry and gas proved to produce a symmetrical singularity spectrum. This means that gas is described by an equal number of points to the left and right side of the  $\alpha_{\text{peak}}$  value or has evenly distributed singularities. Oil on the other hand had an asymmetry of 1.04255. This indicates that oil contains more singularities to the left of its  $\alpha_{\text{peak}}$ . These significant differences between the gas, oil and water singularity spectra were positive results with respect to this study. This is because this means delineating of these reservoir fluids looked possible by performing fractal analysis. Therefore, the study then proceeded to test its detection and delineation method on actual seismic data.

The seismic data obtained from a wild cat well contained 5 gas reservoirs and one oil reservoir. Our detection and delineation technique was using the windowing technique adapted from Khan (2007) and obtaining a singularity spectrum for each window. The detection was done by performing a continuous wavelet transform on the collection of  $\alpha_{\text{peak}}$  values of all the windows. The results indicated the existence of singularities (or high energy regions) at the locations where gas was present. Meanwhile, the oil region was also highlighted as a region with higher energy compared to its surroundings. The continuous wavelet transform seen on figure 41 depicts this clearly.

With the success of the detection phase, the study moved on to the delineation phase where emphasis was given to the other spectral attributes like width and asymmetry on top of  $\alpha_{\text{peak}}$  values. Before going into the results obtained from these attributes, one interesting pattern was observed from our results. The singularity spectrum seems to

move to the left from the window where the reservoir starts to the window where the analysis is within the reservoir. The spectrum then moves back to the right for the window which is related to the end of the reservoir. This means that the spectrum moves to a region of lower  $\alpha$  values when it is within the gas region signalling higher irregularity compared to the surrounding. It then moves to higher  $\alpha$  values as it leaves the high irregularity region pointing towards a reduction in irregularity. This agrees with what we understand about fractal analysis and gases in general. Gases have atoms of high energy and are constantly moving which results in a higher irregularity compared to other zones containing liquids and solids.

Now looking at the spectral attributes for  $\alpha_{\text{peak}}$  and asymmetry, the range of limiting values can be seen as follows:

$$-2.1381 \leq \alpha_{\text{peak}} \leq -1.9958$$

$$0.916025 \leq \text{asymmetry} \leq 1.069975$$

Singularity spectra with spectral attributes within this region of values pointed towards gases. We find that the asymmetry value remains close to the region of 1.0 as we had seen with the results for gases from the seismic modelling. In addition to that, the pattern observed with the width serves as an additional indication on whether we are approaching a gas reservoir. This is because from the results, we have seen that the width of the singularity spectrum of the window decreases from the area where the reservoir starts and as we move into the reservoir.

With the oil reservoir, the same pattern of singularity spectrum movement as seen with gas was observed. The spectrum starts from the right (higher  $\alpha$  values) and moves to the left (lower  $\alpha$  values) as we move into the reservoir – an indication of increase in irregularity as we approach the oil region. Then we also looked at the  $\alpha_{\text{peak}}$  and asymmetry values for delineation:

$$-1.71331 \leq \alpha_{\text{peak}} \leq -1.60587$$

$$1.253554 \leq \text{asymmetry} \leq 1.269845$$

These were the limiting factors for the delineation of oil. The increase in  $\alpha_{\text{peak}}$  values as compared to the  $\alpha_{\text{peak}}$  values is also as expected since oil is in liquid form and is

more regular compared to gas. A similar result had also already been seen in the seismic models. These values indicate the clear possibility of using the spectral attributes to delineate oil as well. However, more tests are definitely needed for the delineation of oil since only one reservoir was tested.

These results, for both the gas reservoirs as well as the oil reservoir were obtained for one wildcat well. Once this algorithm is applied on more wells with hydrocarbons present, the complete range of limiting values for the spectral attributes can be identified to improve the precision of this method.

As a closing remark, the study has proven the detection and delineation is possible when fractal analysis is used together with the windowing technique. This technique could potentially save a lot of time and costs when applied in the field since hydrocarbon detection and delineation can be done directly from seismic data.

## **5.2 Recommendations for future work**

Further work would definitely be needed to increase the reliability and confidence level of using this method. The future works that can be done are:

- The method needs to be applied on more seismic data from real wells to be able to obtain a complete limiting range of values for the spectral attributes to improve delineation reliability.
- The method has to be tested on more oil reservoirs to prove that the detection and delineation method is also reliable on oils as it is for gases. This is because in this study on one oil reservoir was tested due to a lack of seismic data.
- This method applies fractal analysis based on the Wavelet Transform Modulus Maxima method, so future work could test on the other methods in fractal analysis for comparison.

## REFERENCES

- Al Salam, H. A., & Al Baruni, S. (2009). *World oil & gas consumption*. Faculty of Petroleum Engineering, Al Fateh University, Tripoli, Libya.
- Albertin, U., Kapoor, J., Randall, R., Smith, M., Brown, G., Soufleris, C., Whitfield, P., & Dewey, F. (2002). The time for depth imaging. *Oilfield Review*, 14(1), 2-15.
- Arneodo, A., Bacry, E., & Muzy, J. F. (1995, January). *Physica a: statistical mechanics and its applications*. Proceedings of the Third european days of thermodynamics on inhomogeneous phases and pattern formation.
- Avseth, P., Mukerji, T., & Mavko, G. (2005). *Quantitative seismic interpretation : Applying rock physics tools to reduce interpretation risk*. (pp. 168-211). Cambridge, England: Cambridge University Press.
- Backes, A. R., & Bruno, O. M. (2008). *Fractal and multi-scale fractal dimension analysis : a comparative study of bouligand-minkowski method*. (Doctoral dissertation, University of Sao Paulo, Brazil).
- Barnes, A. E., Fink, L., & Laughlin, K. (2004). *Improving frequency domain thin bed analysis*
- Bobrov, N. Y., Smirnova, N. A., Vallianatos, F., & Makris, J. P. St. Petersburg State University, Earth Physics Department. Technological Educational Institute of Crete, Department of Natural Resources and Environment, Department of Electronics. (n.d.). *Multifractal analysis : A method to investigate non-stationary properties of geophysical processes*
- Boschetti, F., Dentith, M. D., & List, R. D. (1996). A fractal-based algorithm for detecting first arrivals on seismic traces. *Society of Exploration Geophysicists*,
- Chakraborty, A., & Okaya, D. (n.d.). Application of wavelet transform to seismic data. 725-728.
- Chhabra, A. B., Meneveau, C., Jensen, R. V., & Sreenivasan, K. R. (1989). Direct determination of the  $f(\alpha)$  singularity spectrum and its application to fully developed turbulence. *The American Physical Society*, 40(9), 5284-5294.
- C.J.G. Evertsz, K. Berkner, W. Berghorn, A local multiscale characterization of edges applying the wavelet transform, in Proc. Nato A.S.I. Fractal Image Encoding and Analysis, Trondheim (1995)

Dansereau, R., & Kinsner, W. (2001). New relative multifractal dimension measures. *IEEE*, 1741-1744.

Devi, S., Cohen, A.J. (2004), *Wavelet Transform and Hybrid Neural Nets for Improved Pore Fluid Prediction and Reservoir Property Estimation*, 10-15 Oct SEG International Exposition and 74<sup>th</sup> Annual Meeting-Denver, Colorado

Ensley, R. (1985). "Evaluation of direct hydrocarbon indicators through comparison of compressional- and shear-wave seismic data: a case study of the Myrnam gas field, Alberta." *GEOPHYSICS*, 50(1), 37-48.

Faghfour, A., & Kinsner, W. (2005). Local and global analysis of multifractal singularity spectrum through wavelets. *IEEE*, 2163-2169.

Fatti, J.L., Smith, G.C., Vail, P.J., Strauss, P.J., & Levitt, P.R. (1994), *Detection of gas in sandstone reservoirs using AVO analysis A 3-D seismic case-history using the Geostack technique*, Society of Exploration Geophysicists

FracLab 2.05 – A Fractal Analysis Software - <http://fracLab.saclay.inria.fr/>

Hall, M., & Trouillot, E. (2004). *Predicting stratigraphy with spectral decomposition*. Paper presented at Cseg national convention, Canada

Hermann, F. J., & Lyons, W. J. (2000). Stratigraphy and lithology classification by singularity analysis.

Jonckheere, I., Nackaerts, K., Muys, B., Aardt, J. V., & Coppin, P. (2006). A fractal dimension-based modelling approach for studying the effect of leaf distribution on lai retrieval in forest canopies. *Ecological Modelling*, 197, 179-195.

Jouck, P. P. H. (2004). Application of the wavelet transform modulus maxima method to t-wave detection in cardiac signals . 1-35.

Khan, M. M. (2007). *Fractal analysis on seismic data for direct detection and delineation of hydrocarbon zones*. (Master's thesis, University of Technology Petronas, Malaysia).

Kinsner, W. (2005). A unified approach to fractal dimensions. *IEEE*, 58-72.

Li, Y., Downton, J. & Xu, Y. (2007), *Practical aspects of AVO modelling*, March edition Leading Edge

Los, C. A., & Yalamova, R. (2006). Multifractal spectral analysis of the 1987 stock market crash. *International Research Journal of Finance and Economics*, (4), 105-132.

Maklad, J.K.D. (2007). *Spectral Detection of Attenuation and Lithology*, CSEG Convention

Makowiec, D., Rynkiewicz, A., Galaska, R., Wdowczyk-Szulc, J., & Zarczynska-Buchowiecka, M. (2011). Reading multifractal spectra: Aging by multifractal analysis of heart rate. *EPL*, 94

Mallat, S., & Wen, L. H. (1992). Singularity detection and processing with wavelets. *IEEE Transactions on Information Theory*, 38(2), 617-643.

Maryam Mahsal Khan, Ahmad Fadzil M.H., M. Firdaus A.H., & Ahmad Riza G. (n.d.). Multifractal analysis of seismic data for delineating reservoir fluids.

Miao, X., Todorovic-Marinic, D., & Klatt, T. (2007). *Enhancing seismic insight by spectral decomposition*. Paper presented at 2007 scpg cseg convention.

Mohamad Hani, A.F (1999). *A/D & D/A Conversion* [PDF Document]. Retrieved from Universiti Teknologi Petronas Digital Signal Processing Class.

Muzy, J.F., Bacry, E., and Arneodo, A., 1993. Multifractal Formalism for fractal Signals: The Structure-function Approach versus the Wavelet Transform Modulus Maxima Method. *Journal of Statistical Physics*, 70(34):635-674.

Polikar, R. (2006). The engineer's ultimate guide to wavelet analysis. *Series of Tutorials to Wavelet Transform*, 1-79.

Reidi, R. H. (n.d.). Multifractal processes. 1-93.

Sohn, H., Robertson, A., & Farrar, C. (2002, August). *Singularity detection using holder exponent*. Proceedings of the US-Korea workshop on smart infrastructural systems, Pusan, South Korea.

Staal (1995), Characterizing the irregularity of measurements by means of wavelet transform, Delft University of Technology

Shengie, S., and Castagna J.P. (2002), *Examples of wavelet transform time-frequency analysis in direct hydrocarbon detection*, Society of Exploration Geophysicists

[Weisstein, E. W.](http://mathworld.wolfram.com/Fractal.html) "Fractal." From *MathWorld*--A Wolfram Web Resource. <http://mathworld.wolfram.com/Fractal.html>

Weisstein, E. W. "Self-Similarity." From *MathWorld*--A Wolfram Web Resource. <http://mathworld.wolfram.com/Self-Similarity.html>

Wilson, T. H. U.S Department of Energy, Morgantown Energy Technology Center. (n.d.). *Fractal interrelationships in field and seismic data*. Morgantown: West Virginia University.

Xiaogui Mia and Scot Cheadle, (1998), *High-resolution seismic data analysis by Wavelet Transform and Matching Pursuit Decomposition*, Veritas, DGC Inc, Society of Exploration Geophysicists

Zia, R. K. P., Redish, E. F., & McKay, S. R. (2007). Making sense of legendre transform.

Zmeskal, O., Vesely, M., Nezadel, M., & Buchnicek, M. (2001). Fractal analysis of image structures. *Harmonic and Fractal Image Analysis*, 3-5.

*Oil and gas background*. (n.d.). Retrieved from [http://www.offshore-sea.org.uk/site/scripts/documents\\_info.php?categoryID=17&documentID=22](http://www.offshore-sea.org.uk/site/scripts/documents_info.php?categoryID=17&documentID=22)

UNEP Industry and Environment, (1997). *Environmental management in oil and gas exploration and production : An overview of issues and management approaches*. Oxford: Words and Publications.

*Discovering the underground structure*. (n.d.). Retrieved from [http://www.oilandgasuk.co.uk/publications/britainsoffshoreoilandgas/Exploration/Discovering the Underground Structure.cfm](http://www.oilandgasuk.co.uk/publications/britainsoffshoreoilandgas/Exploration/Discovering%20the%20Underground%20Structure.cfm)

## APPENDICES

### APPENDIX A – MATLAB CODES

#### Seismic Model Analysis

The following MATLAB code was used for one of the models and changed accordingly for each model:

```
%start of code segment

z=zeros(1,length(n));
z(7)=.21256; %start oil layer
z(17)=-.21256; %end oil layer
z(39)=.21256; % start oil layer
z(59)=-.21256; % end oil layer

figure;
stem(n,z) % produce reflectivity series

f = 60; % centre frequency of Ricker wavelet
n1 = 17;
dt = 0.002;
t0 = 1/f;
T=dt*(n1-1);
t=0:dt:T;
tau = t-t0;

s = (1-2*tau.*tau*f^2*pi^2).*exp(-tau.^2*pi^2*f^2); %Ricker wavelet
eqtn

y=conv(z,s) % convolution of wavelet and reflectivity series
figure;
plot(y)
```

#### Direct Hydrocarbon Detection and Delineation

Codes for upsampling of reflection coefficients for windowing:

```
%start of code segment

%y = Reflection Coefficients
%y1 = Reflection Coefficients + convolution
%y2 = Upsampled version of y1

y= Reflection_coefficients;
x=[1:0.004:3.156];
figure;
plot(x,y);
```

```

f = 60;
n1 = 17;
dt = 0.002;
t0 = 1/f;
T=dt*(n1-1);
t=0:dt:T;
tau = t-t0;

s = (1-2*tau.*tau*f^2*pi^2).*exp(-tau.^2*pi^2*f^2);
y1=conv(y,s);
x1=[1:0.004:3.220];

figure;
plot(x1,y1);
title('Seismic Trace');
ylabel('Amplitude');
xlabel('msec');

y2 = resample (y1,20,1); %upsampling
x2=[1:0.0002:3.2238];
figure;
plot(x2,y2);
title('Upsampled Seismic Trace');
ylabel('Amplitude');
xlabel('msec');

```

Codes for one window, which is then done for every window:

```

%start of code segment
>window 1
%40 samples (y) in each window
%fractal analysis is performed on each window on FracLab

x = [1:0.0002:1.0078];
y = resampled_window1;

figure;
plot(x,y);

```